sustainability

MDPI

Article

Spatial Inequality and Infrastructure-Based Carbon Lock-In in Green Logistics: Evidence from China

Hao Zhang [1], Zhonghua Xu [2,*], Peng Wang [2] and Jie He [3]

[1] Faculty of Management Engineering, Huai'an University, Huai'an 223003, China; zhhao@hyit.edu.cn
[2] Faculty of Transportation Engineering, Huai'an University, Huai'an 223003, China; 19851397237@139.com
[3] School of Transportation, Southeast University, Nanjing 210096, China; hejie@seu.edu.cn
* Correspondence: 212409610804@hyit.edu.cn

Abstract

The logistics industry remains a critical bottleneck for decarbonization due to its extensive physical networks and high-carbon path dependencies. To address the spatial heterogeneity and transition constraints in the logistics industry of China, this study proposes a Performance–Topology–Mechanism (PTM) framework. Analyzing panel data from 30 Chinese provinces, we integrate a Super-SBM model with the Global Malmquist–Luenberger (GML) index, Dagum Gini decomposition, and a panel Tobit model to decode the spatiotemporal dynamics of green innovation performance (GIP) and its underlying spatial lock-in mechanisms. The results reveal a steady but spatially uneven increase in the national GIP (from 0.4526 to 0.5724), characterized by a leading East and a lagging West/Northeast. GML decomposition indicates this growth is predominantly driven by outward shifts in the technological frontier rather than efficiency improvements, highlighting the weak spatial conversion of green technologies into transport optimization. Topological tracing demonstrates that inter-regional disparities have become the dominant source of spatial inequality, with their contribution rising from 60% to 75%. Spatial autocorrelation further exposes a deepening core–periphery polarization and persistent low-performance spatial lock-in. Crucially, the mechanism analysis identifies a pronounced infrastructure-based carbon lock-in. While economic capacity and green patents stimulate GIP, road network density exerts a significant negative effect, reflecting a systemic path dependence on high-carbon road freight. The findings suggest that decarbonizing transport logistics requires shifting from singular technological investments toward multimodal transport restructuring, overcoming physical network dependencies, and promoting the regional diffusion of green innovations. These findings provide an empirical basis for differentiated green-logistics policies, coordinated low-carbon transport infrastructure planning, and cross-regional diffusion of green technologies.

Keywords: green logistics; spatial inequality; infrastructure-based carbon lock-in; Dagum Gini decomposition; spatiotemporal dynamics

Check for updates

Received: 13 July 2026
Revised: 13 August 2026
Accepted: 17 August 2026
Published: 19 August 2026

Copyright: © 2026 by the authors. Licensee MDPI, Basel, Switzerland. This article is an open access article distributed under the terms and conditions of the Creative Commons Attribution (CC BY) license.

1. Introduction

Driven by the global energy transition and carbon neutrality goals, breaking carbon lock-in in energy-intensive industries has become a key issue in energy economics. The IEA [1] reports that global energy-related carbon emissions reached 37.8 billion tons in 2024. Large-scale clean technology deployment now avoids about 2.6 billion tons of emissions each year. The share of oil in global energy demand has also fallen below 30% for the

first time. However, transport and logistics remain a major barrier to emission reduction. Road transport accounts for more than 70% of transport-sector carbon emissions. As the backbone of logistics, road freight is therefore central to decarbonization [2]. E-commerce logistics may also reduce pollution by replacing some individual shopping trips with consolidated deliveries, although its net environmental benefit depends on the efficiency of last-mile operations [3].

Beyond aggregate emission reduction, the green transition also raises an issue of spatial and infrastructural equity. At the international policy level, the European Green Deal calls for a just and inclusive transition, while the UN 2030 Agenda links sustainable and resilient infrastructure with inclusive economic development, reduced inequality, accessible transport, and climate action through SDGs 9, 10, 11, and 13 [4,5]. Unequal access to transport networks, logistics hubs, and low-carbon technologies can concentrate economic opportunities in well-connected regions while increasing transport disadvantage and social exclusion in peripheral areas [6,7]. Against this background, China faces a particularly pressing logistics decarbonization challenge. As the world's largest logistics market, transport and logistics generate nearly 15% of China's carbon emissions, nearly 80% of which come from road freight [8]. China also accounts for two-thirds of global electric vehicle sales. It has achieved its 2030 wind and solar capacity targets six years ahead of schedule [9,10]. Even so, the extensive growth model of road freight has not changed fundamentally. Transport infrastructure creates strong path dependence, and unequal network connectivity and spatial accessibility may reinforce regional differences in low-carbon mobility and logistics transition capacity [11,12]. Therefore, traditional extensive management is no longer sufficient. A key breakthrough is to measure logistics green innovation performance (GIP) accurately. It is also necessary to examine its spatiotemporal evolution and driving mechanisms. This can support more precise regional energy policies and low-carbon transport planning.

Although energy efficiency and green innovation have been widely discussed, logistics remains underexplored. It is a highly energy-intensive network system. Existing studies still show three main gaps.

First, efficiency measurement and dynamic tracking remain insufficient. Logistics GIP evaluation should consider both resource allocation and undesirable outputs. Traditional radial DEA models ignore slack variables. This may lead to biased efficiency results [13]. Tone's Super-SBM model solves this problem. It can handle slack variables and undesirable outputs [14]. However, many studies still use it only for static evaluation. Wu et al. [15] and Zhao et al. [16] measured green logistics efficiency and transport carbon efficiency. Yet they did not capture intertemporal change. The global Malmquist–Luenberger (GML) index proposed by Oh [17] is useful for dynamic productivity analysis. Hamid et al. [18] and Ge et al. [19] used it to study industrial green productivity. Yi et al. [20] further combined GML with Super-SBM. Their study showed that this combination can separate technical efficiency from technological progress. However, this integrated approach is still rare in logistics GIP research. Some related studies focus on transport carbon emissions rather than green logistics innovation [21]. Others still separate static and dynamic logistics-efficiency analysis [22]. Addis et al. [23] also noted that evaluation frameworks are limited if they lack slack adjustment and a global production possibility set. Thus, integrating Super-SBM and GML is important for capturing logistics GIP more completely.

Second, the spatial sources of inequality have not been clearly identified. Logistics is a physical network across geographic space. Its GIP depends not only on technology. It is also shaped by economic agglomeration, infrastructure dependence, spatial heterogeneity, and spillover effects [24]. Common measures include the Theil index and the coefficient of variation. However, these methods cannot handle overlapping sample distributions

well. This may cause measurement bias [25]. The Dagum Gini decomposition method offers a better solution. Wang et al. [26] and Gao et al. [27] show that it can identify the spatial structure of carbon-emission disparities more precisely. It separates intra-regional disparities, inter-regional net disparities, and transvariation density. Jiao et al. [28] applied this method to logistics carbon emissions. This confirms its potential in logistics research. However, studies on logistics GIP still often use the coefficient of variation or Theil index [29]. They also tend to ignore overlapping regional distributions [30]. Some studies have examined green innovation performance, carbon emission efficiency, and carbon networks with spatial methods [31–33]. Yet few extend Dagum decomposition to logistics GIP. Li et al. [34] therefore argue that regional inequality in green logistics innovation should be traced through Dagum Gini decomposition.

Third, the driving mechanisms of logistics GIP remain unclear. There are also econometric problems. Super-SBM efficiency values are bounded dependent variables. If Ordinary Least Squares is used directly, the estimated parameters may be biased [35]. Tobit or truncated regression is more suitable for two-stage DEA efficiency analysis [36]. Many studies have followed this approach. Deng et al. [37] and Liu et al. [38] used Tobit models to examine green transport and logistics efficiency. However, scholars still disagree on the effects of key factors. For road-network density, Driscoll et al. [39] found a carbon lock-in effect. They argued that road expansion may lock logistics into a high-carbon path. It may also reduce green efficiency. Dong et al. [40] and Zhang et al. [41] reached similar conclusions. For R&D investment, Hao et al. [42] proposed a "green paradox." Under resource misallocation, higher R&D expenditure may not promote green innovation. It may even create structural inhibition. Wang et al. [43], Zhou et al. [44], and Qiu et al. [33] also found complex spatial and paradoxical effects of technological innovation. The effects of environmental regulation and economic development are also debated. Yao et al. [45,46] found threshold effects of regulation. They also found nonlinear links between economic development and green logistics efficiency. Moktadir et al. [47] stressed the need for empirical clarification within a unified framework.

To address these gaps, this study builds a Performance–Topology–Mechanism (PTM) framework. It examines logistics GIP in 30 Chinese provinces from 2013 to 2022. Hong Kong, Macao, Taiwan, and Tibet are excluded. The study makes three contributions. First, it combines the undesirable-output Super-SBM model with the GML index. This creates an integrated static–dynamic evaluation system. It reduces slack-variable bias and avoids spurious technological regression. It also supports static ranking and dynamic decomposition of total factor productivity. Second, it introduces Dagum Gini decomposition and Moran's I. This helps trace spatial imbalance and identify the main sources of regional inequality in logistics GIP. Third, it uses a random-effects panel Tobit model. This model is suitable for bounded dependent variables. It improves the robustness of mechanism identification. It also provides evidence for optimizing energy infrastructure and correcting technological-factor misallocation.

The remainder of this paper is organized as follows. Section 2 introduces the PTM framework, study sample, data, indicator system, and empirical methods. Section 3 presents the GIP measurement, dynamic decomposition, spatial analysis, mechanism analysis, robustness tests, and endogeneity test. Section 4 summarizes the conclusions, policy implications, research limitations, and future research directions.

2. Materials and Methods

2.1. Performance–Topology–Mechanism Analytical Framework

To systematically examine the green innovation performance (GIP) of China's logistics industry, this study develops an integrated Performance–Topology–Mechanism

(PTM) framework that connects efficiency dynamics, spatial differentiation, and structural constraints through a common province-level GIP measure. The Performance dimension measures static efficiency and decomposes intertemporal productivity change into technical efficiency change and technological progress. Based on these results, the Topology dimension identifies whether performance improvements are spatially shared or concentrated by decomposing regional inequality and detecting spatial agglomeration and lock-in. The Mechanism dimension subsequently examines how infrastructure dependence, resource allocation, and green technology conversion are associated with the identified performance and spatial patterns, as shown in Figure 1.

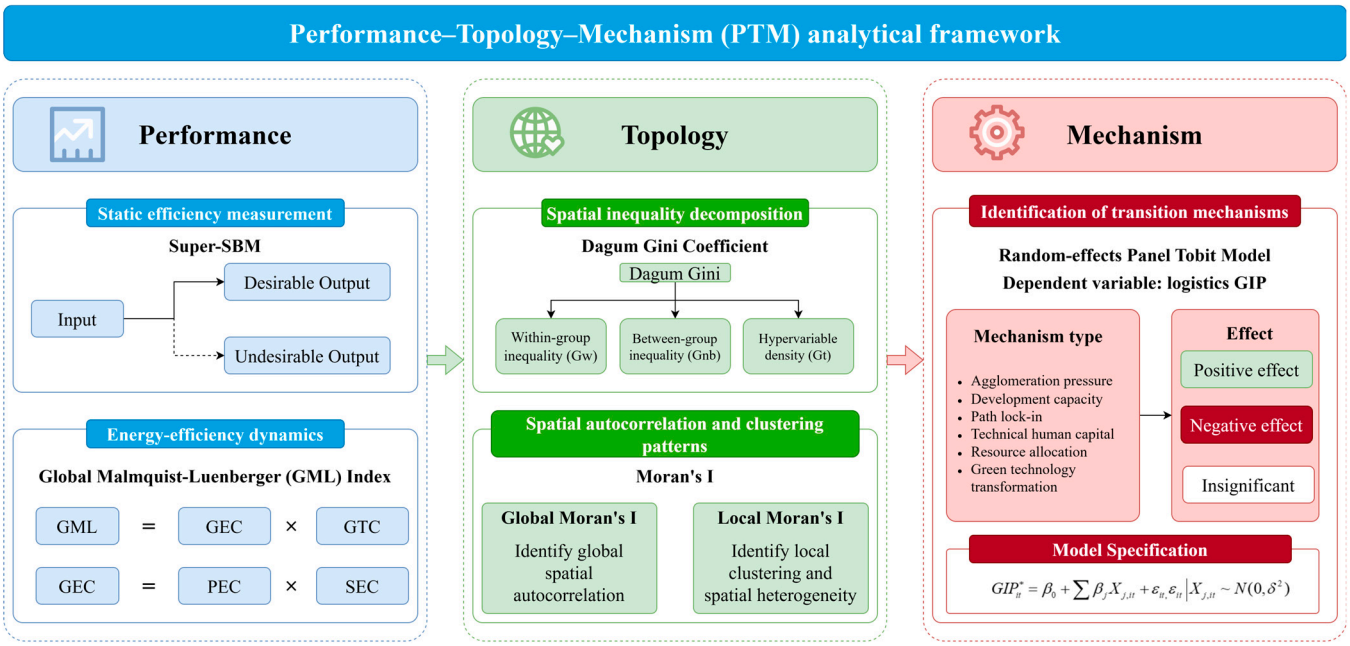


Figure 1. Performance–Topology–Mechanism (PTM) Integrated Analysis Framework.

(1) **Performance.** This dimension aims to measure the static efficiency level of logistics GIP and its dynamic changes in energy efficiency. First, the Super-SBM model incorporating undesirable outputs is used to measure logistics GIP in each province, thereby identifying the relative efficiency of different regions in input utilization, desirable output expansion, and carbon pollution reduction. Second, the global Malmquist–Luenberger (GML) index based on the global production possibility set is introduced to decompose changes in GIP into green technical efficiency change, green technological progress change, pure technical efficiency change, and scale efficiency change, so as to determine the sources of GIP improvement.

(2) **Topology.** This dimension aims to reveal the sources of spatial inequality in logistics GIP and its agglomeration patterns. Given the strong geographical proximity, infrastructure dependence, and regional interconnectivity of the logistics industry, this study employs the Dagum Gini coefficient and its decomposition method to divide overall spatial inequality into intraregional disparities, interregional disparities, and transvariation density, thereby identifying the main sources of inequality. Furthermore, global and local Moran's I indices are used to analyze the spatial correlation, agglomeration types, and low-performance lock-in areas of logistics GIP.

(3) **Mechanism.** This dimension aims to explain the formation mechanisms of logistics GIP disparities and carbon lock-in. Based on the Tobit model, this study identifies the key factors affecting logistics GIP from six aspects, as follows: agglomeration pressure, development capacity, path lock-in, technological human capital, resource allocation,

and green technology conversion. Particular attention is paid to whether road network density reinforces dependence on road freight and thereby creates infrastructure-based carbon lock-in, and whether R&D investment suffers from resource misallocation that is inconsistent with green transition objectives.

The PTM framework links the sources, spatial distribution, and structural constraints of changes in GIP. This integration distinguishes a broadly shared regional green transition from a development pattern characterized by technological-frontier expansion, weak efficiency conversion, and spatially concentrated gains, thereby providing a unified analytical basis for explaining why productivity improvement may coexist with regional inequality and infrastructure-based carbon lock-in. The framework is also modular and methodologically replicable. Comparable decision-making units and locally available indicators can be used in other countries or transport sectors while retaining the same sequence of performance measurement, dynamic decomposition, spatial analysis, and mechanism testing.

2.2. Study Area and Data Sources

2.2.1. Definition of the Study Area and Spatial Division

Considering administrative continuity, provincial-level statistical comparability, and data availability, this study selects 30 provincial-level regions in mainland China, excluding Hong Kong, Macao, Taiwan, and Tibet, as the spatial sample for the empirical analysis. The study period covers 2013–2022. To capture the spatial heterogeneity and regional coordination characteristics of logistics GIP, this study develops an analytical functional classification based on national regional development strategies and the pole–cluster–group hierarchy of China's national comprehensive transport network. The classification further considers spatial contiguity, logistics-hub functions, transport infrastructure endowments, and regional low-carbon transition conditions [48–54]. It is a study-specific analytical grouping rather than an official administrative division. Accordingly, the 30 provincial-level regions are divided into seven functional regions, as follows: the Eastern Leading-Type Region (EL-TR), Central Emerging Region (CER), Western Core Growth Pole Region (WCGPR), Western Accelerated Development Region (WADR), Northern Optimized Development Region (NODR), Northeastern Revitalization Region (NRR), and Featured Development Region (FDR). The provincial composition and classification rationale of each region are reported in Table A1.

2.2.2. Data Sources and Core Variable Processing

The data were mainly obtained from the *China Statistical Yearbook*, *China Energy Statistical Yearbook*, *China Environmental Statistical Yearbook*, *China Statistical Yearbook on Science and Technology*, *China Transportation Statistical Yearbook*, and *provincial statistical yearbooks* and *statistical communiqués*. Table 1 reports the definitions, units, calculation methods, data transformations, and sources of all GIP indicators.

Missing values were confined to the value added of the transport, storage, and postal sector for all provinces in 2018. This missingness was mainly associated with adjustments in statistical definitions during China's Fourth National Economic Census. The missing observations were imputed using multiple imputation by chained equations (MICE). All monetary variables were converted to 2013 constant prices. Fixed-asset investment was deflated using the fixed-asset investment price index, while sectoral value added and technology-market transaction values were deflated using the corresponding provincial price indices.

Table 1. Evaluation Index System of Green Innovation Performance in Logistics Industry.

Type	Primary Indicator	Secondary Indicator	Variable Definition or Calculation Formula	Unit	Attr.
Input indicators	Human Resources Investment	Industry Employment Scale	L_{it} = number of persons employed in urban units in the transport, storage, and postal sector	10^4 persons	+
		High-quality Talent Reserve	$H_{it} = L_{it}^{info} / L_{it}^{total} \times 100$, where L^{info} is employment in information transmission, software, and information technology services and L^{total} is total provincial employment	%	+
	Capital and Facility Investment	Fixed Asset Investment	$I_{it}^r = I_{it}^n / (P_{it}^{FAI}/100)$, where I^n is nominal fixed-asset investment and P^{FAI} is the fixed-asset investment price index	CNY 100 million, 2013 constant prices	+
		Fixed Asset Stock	$K_{it} = (1-\delta)K_{i,t-1} + I_{it}^r$, where $\delta = 10.96\%$; $K_{i0} = I_{i0}^r / (g_i + \delta)$	CNY 100 million, 2013 constant prices	+
		Green Facility Foundation	$R_{it} = R_{it}^{raw} \times 10,000$, where R^{raw} is railway mileage reported in 10^4 km	km	+
		Digital Infrastructure	$F_{it} = F_{it}^{raw} \times 10,000$, where F^{raw} is the length of long-distance fiber-optic cable lines reported in 10^4 km	km	+
	Energy and Innovation Environment	Total Energy Consumption	$EC_{it} = \sum_j E_{ijt}\theta_j$, where E_{ijt} is consumption of energy type j and θ_j is its standard-coal conversion coefficient	10^4 tonnes of standard coal	+
		Optimization of Energy Structure	EL_{it} = electricity consumption	10^8 kWh	+
		Enterprise Website Penetration Rate	$WEB_{it} = N_{it}^{website} / N_{it}^{enterprise} \times 100$, WEB_{it} where is the enterprise website penetration rate, $N_{it}^{website}$ is the number of websites owned by enterprises, and $N_{it}^{enterprise}$ is the total number of enterprises.	%	+
		Informatization Level	$INF_{it} = N_{it}^{mobile} / POP_{it} \times 100$, where INF_{it} is the informatization level, N_{it}^{mobile} is the number of mobile phone subscriptions, and POP_{it} is the permanent resident population.	subscriptions per 100 persons	+
Expected Output Indicators	Economic Benefits	Industry Economic Scale	$Y_{it}^r = Y_{it}^n / (P_{it}^Y/100)$, where Y^n is nominal value added in the transport, storage, and postal sector and P^Y is the corresponding price index	CNY 100 million, 2013 constant prices	+
		Economic Output Efficiency	$LP_{it} = Y_{it}^r / L_{it}$, where LP_{it} is economic output efficiency, Y_{it}^r is the real value added of the transport, storage, and postal sector at 2013 constant prices, and L_{it} is employment in this sector.	CNY 10,000 per person	+
	Service and Operational Efficiency	Freight Service Efficiency	$FS_{it} = FT_{it} / POP_{it}$, where FT is total freight turnover and POP is permanent resident population	10^4 tonne-km per person	+
		Facility Utilization Efficiency	$FU_{it} = RFT_{it} / RM_{it}$, where RFT is road freight turnover and RM is road mileage	10^4 tonne-km per km	+
		Greening of Transportation Structure	$GS_{it} = RFT_{it}^{rail} / FT_{it} \times 100$, where GS_{it} is the greening of transportation structure, RFT_{it}^{rail} is railway freight turnover, and FT_{it} is total freight turnover.	%	+

Table 1. *Cont.*

Type	Primary Indicator	Secondary Indicator	Variable Definition or Calculation Formula	Unit	Attr.
Expected Output Indicators	Innovation Benefits	Innovation Achievement Absorption Efficiency	$IA_{it} = TM^r_{it}/L_{it}$, where TM^r is the real technology-market transaction value	CNY 10,000 per 10,000 persons	+
		Industrial Collaborative Development	$IC_{it} = Y^r_{it}/GDP^r_{it} \times 100$, where IC_{it} is industrial collaborative development, Y^r_{it} is the real value added of the transport, storage, and postal sector, and GDP^r_{it} is real regional GDP, both measured at 2013 constant prices.	%	+
		Technology Transaction	$TM^r_{it} = TM^n_{it}/(P^{GDP}_{it}/100)$, where TM^n is the nominal technology-market transaction value	CNY 10,000, 2013 constant prices	+
Non-expected output indicators	Carbon Emissions	CO_2 Emissions Volume	$CO_{2,it} = \sum_j E_{ijt} \times NCV_j \times CC_j \times OF_j \times 44/12$, where NCV is the net calorific value, CC is the carbon content per unit of calorific value, and OF is the oxidation factor	10^4 tonnes	−
		Carbon Emission Intensity	$CI_{it} = CO_{2,it}/Y^r_{it}$, where CI_{it} is carbon emission intensity, $CO_{2,it}$ is CO_2 emissions from the transport, storage, and postal sector, and Y^r_{it} is the real value added of this sector at 2013 constant prices.	tonnes per CNY 10,000	−
	Conventional Air Pollution	Total Pollutant Emissions Volume	NOX_{it} = total nitrogen oxides emissions from the transport, storage, and postal sector	10^4 tonnes	−
		Pollutant Emission Intensity	$NI_{it} = NOX_{it}/FT_{it} \times 10{,}000$, where NI_{it} is pollutant emission intensity, NOX_{it} is total NOx emissions from the transport, storage, and postal sector, and FT_{it} is total freight turnover. The factor 10,000 converts NOx emissions from 10^4 tonnes to tonnes.	tonnes per 10^8 tonne-km	−

Note: "+" and "−" denote positive and negative indicators, respectively. CO_2 and NOx represent carbon emissions and conventional air pollution, respectively. In all formulas, i denotes province and t denotes year.

Fixed-capital stock was estimated using the perpetual inventory method, with the depreciation rate set at 10.96%. CO_2 emissions were calculated by energy type using energy consumption and the net calorific values, carbon contents per unit of calorific value, and oxidation factors recommended by the IPCC. NOx emissions were obtained from environmental statistical sources and used to measure conventional air pollution. The corresponding calculation formulas are presented in Table 1.

2.3. Evaluation Indicator System for Logistics GIP

Based on the connotation of green innovation and relevant studies on green innovation, transport carbon efficiency, and logistics eco-efficiency [15,22,37,45,46], this study constructs an environmental-economic logistics GIP evaluation system comprising inputs, desirable outputs, and undesirable outputs. Digital-support inputs can promote green innovation through resource allocation, information sharing, and innovation cooperation [55–57]. Accordingly, Enterprise Website Penetration Rate and Informatization Level are used to measure digital support capacity. The undesirable outputs include both CO_2 emissions and NOx pollution, representing carbon emissions and conventional air pollution, respectively. The definitions, units, and calculation methods of all indicators are presented in Table 1.

2.4. Analytical Methods for the Performance Dimension

2.4.1. Super-SBM Model

To overcome the limitations of traditional DEA models, which ignore slack variables, fail to handle undesirable outputs, and cannot distinguish among efficient decision-making units, this study adopts the Super-SBM model with undesirable outputs proposed by Tone, K [14]. This model can eliminate slack bias, incorporate undesirable outputs, and allow efficiency scores to exceed 1, thereby enabling a more accurate ranking and comparison of logistics GIP across the 30 provinces.

Suppose there are n Decision Making Units (DMU). Each DMU consists of m inputs, s_1 expected outputs, and s_2 undesirable outputs, represented by vectors $x \in R^m, y^g \in R^{s_1}$, and $y^b \in R^{s_2}$, respectively.

$$X = [x_1, \ldots, x_n] \in R^{m \times n} \tag{1}$$

$$Y^g = \left[y_1^g, \ldots, y_n^g\right] \in R^{s_1 \times n} \tag{2}$$

$$Y^b = \left[y_1^b, \ldots, y_n^b\right] \in R^{s_2 \times n} \tag{3}$$

For a specific $DMU_k(x_k, y_k^g, y_k^b)$, the programming formulation of the Super-SBM model considering undesirable outputs is presented as follows:

$$\rho^* = \min \frac{\frac{1}{m}\sum_{i=1}^{m}\frac{\overline{x}_i}{\overline{x}_{ik}}}{\frac{1}{s_1+s_2}\left(\sum_{r=1}^{s_1}\frac{\overline{y}_r^g}{y_{rk}^g} + \sum_{t=1}^{s_2}\frac{\overline{y}_t^b}{y_{tk}^b}\right)} \tag{4}$$

$$s.t.\begin{cases} \overline{x}_i \geq \sum\limits_{\substack{j=1 \\ j \neq k}}^{n} \lambda_j x_{ji}^b \\ \overline{y}_r^g \leq \sum\limits_{\substack{j=1 \\ j \neq k}}^{n} \lambda_j y_{jr}^g \\ \overline{y}_t^b \geq \sum\limits_{\substack{j=1 \\ j \neq k}}^{n} \lambda_j y_{jt}^b \\ \overline{x}_i \geq x_{ik}, \overline{y}_r^g \leq y_{rk}^g, \overline{y}_t^b \geq y_{tk}^b \\ \lambda_j \geq 0 \end{cases} \tag{5}$$

where ρ^* represents the GIP value of the logistics industry; λ_j denotes the weight vector; and $\overline{x}, \overline{y}^g, \overline{y}^b$ correspond to the target values for inputs, desirable outputs, and undesirable outputs, respectively.

2.4.2. Global Malmquist–Luenberger Index and Its Decomposition

To investigate the dynamic evolution and driving effects of logistics GIP, this study introduces the global Malmquist–Luenberger (GML) index model proposed by Oh [17], building on the static measurement results obtained from the Super-SBM model. We are assuming that all input-output data from the entire study period T spanning 2013–2022 constitutes a global baseline technology set $P^G(x)$, defined as follows:

$$P^G(x) = P^1(x) \cup P^2(x) \cup \ldots \cup P^t(x) \tag{6}$$

Accordingly, the directional distance function based on global technology, $\overrightarrow{D}^G$, is defined as follows:

$$\overrightarrow{D}^G\left(x^t, y^t, b^t; g_y, -g_b\right) = \sup\left\{\boldsymbol{\beta} \geq \mathbf{0} : \left(x^t, y^t + \beta g_y, b^t - \beta g_b\right) \in P^G\right\} \tag{7}$$

where $g = (g_y, -g_b)$ is the directional vector, with $g_y \geq 0$ and $g_b \geq 0$. $\beta \geq 0$ represents the maximum feasible expansion of desirable outputs and simultaneous contraction of undesirable outputs, while inputs remain unchanged. This restriction ensures that the directional distance function is non-negative, making the interpretation of the GML index in Equation (8) consistent, as follows: GML > 1, GML < 1, and GML = 1 indicate performance growth, decline, and no change, respectively.

Based on the aforementioned distance function, the GML index of logistics green innovation performance from period t to period $t+1$ is defined as follows:

$$GML^{t,t+1} = \frac{1 + D^G(x^t, y^t, b^t)}{1 + D^G(x^{t+1}, y^{t+1}, b^{t+1})} \tag{8}$$

Regarding this index, if $GML^{t,t+1} > 1$, it indicates that from period t to $t+1$, the GIP of the logistics industry in the province has achieved growth. Conversely, if $GML^{t,t+1} < 1$, a decline is signified; if $GML^{t,t+1} = 1$, the performance is shown to remain unchanged.

To deeply analyze the intrinsic drivers of performance variations, the GML index is further decomposed into Green Technical Efficiency Change (GEC) and Green Technical Progress Change (GTC), as follows:

$$\begin{aligned} GML^{t,t+1} &= GEC^{t,t+1} \times GTC^{t,t+1} \\ GEC^{t,t+1} &= \frac{1+D^t(x^t,y^t,b^t)}{1+D^{t+1}(x^{t+1},y^{t+1},b^{t+1})} \\ GTC^{t,t+1} &= \frac{GML^{t,t+1}}{GEC^{t,t+1}} \end{aligned} \tag{9}$$

The function is further decomposed as follows:

$$\begin{aligned} GEC^{t,t+1} &= PEC^{t,t+1} \times SEC^{t,t+1} \\ PEC^{t,t+1} &= \frac{1+D^t\left(x^t,y^t,b^t\right)}{1+D_{vrs}^{t+1}\left(x^{t+1},y^{t+1},b^{t+1}\right)} \\ SEC^{t,t+1} &= \frac{GEC^{t,t+1}}{PEC^{t,t+1}} \end{aligned} \tag{10}$$

where GEC is the change in green technological efficiency, reflecting the extent to which the decision-making unit approaches the current optimal frontier and signifying improvements in management standards and resource allocation capabilities; GTC is the change in green technological progress, reflecting shifts in the technological frontier itself; PEC is the change in pure technological efficiency, reflecting changes in the decision-making unit's efficiency in management and technological application; SEC is the change in scale efficiency, reflecting whether the decision-making unit is moving towards an optimal production scale.

2.5. Analytical Methods for the Topology Dimension

2.5.1. Dagum Gini Coefficient and Subgroup Decomposition

To reveal the spatial imbalance characteristics and underlying causes of logistics GIP in China, this study employs the Dagum Gini coefficient decomposition method [25].

Let G denote the overall Gini coefficient, which is used to measure the degree of overall disparity in logistics GIP across the country. The calculation formula is as follows:

$$G = \frac{\sum_{j=1}^{k}\sum_{h=1}^{k}\sum_{i=1}^{n_j}\sum_{r=1}^{n_h}\left|y_{ji} - y_{hr}\right|}{2 \cdot n^2 \cdot \overline{y}} \tag{11}$$

where $y_{ji}(y_{hr})$ denotes the logistics GIP value of the $i(r)$-th province in the $j(h)$-th region; $\overline{y}$ represents the national average logistics GIP; n denotes the number of provinces; k

denotes the number of divided regions; and $n_j(n_h)$ represents the number of provinces in the $j(h)$-th region.

According to the Dagum decomposition method, the overall Gini coefficient G is decomposed into three components, as follows:

$$\begin{aligned} G &= G_w + G_{nb} + G_t \\ G_w &= \sum_{j=1}^{k} G_{jj} \cdot p_j \cdot s_j \\ G_{nb} &= \sum_{j=2}^{k} \sum_{h=1}^{j-1} G_{jh}\left(p_j s_h + p_h s_j\right) D_{jh} \\ G_t &= \sum_{j=2}^{k} \sum_{h=1}^{j-1} G_{jh}\left(p_j s_h + p_h s_j\right)\left(1 - D_{jh}\right) \end{aligned} \tag{12}$$

where G_w denotes the contribution of intraregional disparities, reflecting differences in performance levels among provinces within each region. G_{jj} is the Gini coefficient of region j, $p_j = n_j/n$ and $s_j = (n_j\overline{y}_j)/(n\overline{y})$. G_{nb} denotes the contribution of interregional disparities, reflecting differences in performance levels among different regional blocks. G_{jh} is the Gini coefficient between regions j and h, and D_{jh} represents the relative influence and its direction. G_t denotes the contribution of transvariation density, reflecting the impact of cross-overlapping phenomena among regions on overall disparities.

2.5.2. Spatial Autocorrelation Analysis

To examine the spatial agglomeration and spillover effects of logistics GIP across Chinese provinces, this study employs spatial autocorrelation analysis. Specifically, the global Moran's I is used to assess overall spatial dependence, while the local Moran's I and Moran scatter plots are applied to identify specific agglomeration patterns and spatial heterogeneity. Considering that spillover effects in the logistics industry mainly rely on geographical proximity and transport connectivity, this study constructs a geographical adjacency weight matrix W_{ij}.

$$W_{ij} = \begin{cases} 1, & \text{If province } i \text{ is geographically adjacent to province } j \\ 0, & \text{If province } i \text{ and province } j \text{ are not geographically adjacent or } i = j \end{cases} \tag{13}$$

$$\begin{aligned} I &= \frac{n\sum_{i=1}^{n}\sum_{j=1}^{n} W_{ij}(x_i - \overline{x})(x_j - \overline{x})}{\sum_{i=1}^{n}\sum_{j=1}^{n} W_{ij}\sum_{i=1}^{n}(x_i - \overline{x})^2} \\ I_i &= \frac{n(x_i - \overline{x})\sum_{j=1}^{n} W_{ij}(x_j - \overline{x})}{\sum_{i=1}^{n}(x_i - \overline{x})^2} \end{aligned} \tag{14}$$

where I is the global Moran's I, n is the total number of provinces, x_i, x_j denote the logistics GIP values of provinces i and j, $\overline{x}$ is the mean logistics GIP, W_{ij} represents the element of the spatial weight matrix based on geographical adjacency, and I_i is the local Moran's I. The global Moran's I takes values in the interval [−1,1].

2.6. Analytical Methods for the Mechanism Dimension

Given that logistics GIP measured by the Super-SBM model is a bounded dependent variable truncated above zero, directly applying OLS may lead to biased and inconsistent estimates. Therefore, this study draws on the Tobit model proposed by Tobin [58] and incorporates a random-effects panel specification to address the data truncation problem.

This approach also makes full use of the long-panel data characteristics of the 30 provinces for the analysis of influencing factors.

$$GIP_{it}^{*} = \alpha + \sum_{j=1}^{J} \beta_j X_{jit} + u_i + \varepsilon_{it},\ u_i \sim N(0, \sigma_u^2),\ \varepsilon_{it} \sim N(0, \sigma_\varepsilon^2) \tag{15}$$

$$GIP_{it}^{*} = \begin{cases} GIP_{it}, if\ GIP_{it} > 0 \\ 0, if\ GIP_{it} \leq 0 \end{cases} \tag{16}$$

where i denotes the province, t denotes the year, and $j = 1, \ldots, J$ indexes the explanatory variables. GIP_{it}^{*} is the latent logistics GIP, while GIP_{it} is the observed value. α is the intercept term, X_{jit} denotes the j-th explanatory variable, and β_j is its corresponding regression coefficient. u_i represents the province-specific random effect, and ε_{it} is the idiosyncratic error term.

3. Results and Analysis

3.1. Evaluation of Green Innovation Efficiency in the Logistics Industry

3.1.1. Static Efficiency Evaluation

Considering the undesirable output indicators of carbon emissions and environmental pollution, logistics GIP is calculated according to Equations (1)–(5). Since provinces differ in their levels of economic development and thus have different production frontiers, it is necessary to calculate the Super-SBM efficiency values for each region over ten periods in order to accurately analyze the annual situation. The logistics GIP of 30 Chinese provinces from 2013 to 2022 is shown in Figures A1 and 2.

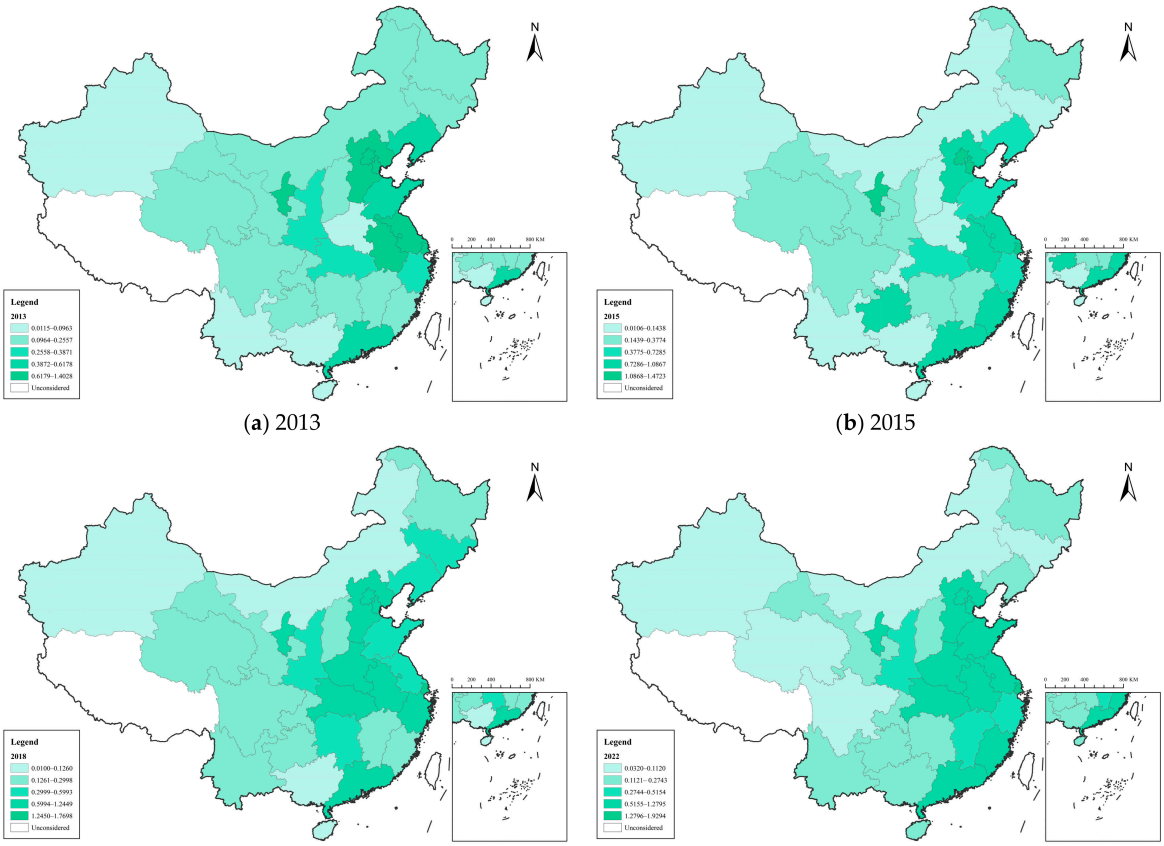


Figure 2. Distribution Map of GIP in the Logistics Industry in 30 Provinces of China, 2013–2022.

As shown in Figures A1 and 2, logistics GIP across the 30 Chinese provinces exhibited a fluctuating upward trend from 2013 to 2022. The national average increased from 0.4526 in 2013 to 0.5268 in 2015 and 0.5458 in 2018, before temporarily declining to 0.5063 in 2020. It subsequently recovered to 0.5576 in 2021 and reached a decade-high value of 0.5724 in 2022. The number of provinces with GIP values equal to or greater than 1 also increased from seven in 2013 to twelve in 2022, indicating a gradual expansion of the provincial efficiency frontier. Nevertheless, the improvement was spatially uneven. Shanghai and Tianjin maintained clear leading positions, with ten-year average values of 1.6481 and 1.2354, respectively. Several central provinces showed evident catch-up trends, as follows: Henan increased from 0.0749 in 2013 to 1.0334 in 2022, while Hubei rose from 0.3490 to 1.0004. By contrast, persistent low values were observed in parts of western and northeastern China. Liaoning declined from 0.4819 to 0.2743, Jilin from 0.1524 to 0.0565, and Inner Mongolia from 0.2138 to 0.0494. Some provinces also experienced nonlinear fluctuations. For example, Zhejiang increased from 0.3270 in 2013 to 1.0189 in 2018, but subsequently declined to 0.5154 in 2022. Overall, the evolution of logistics GIP was characterized by national improvement, a stable high-performance core, the emergence of central catch-up provinces, persistent low-performance areas, and considerable provincial volatility.

To further characterize the temporal evolution and regional differentiation of provincial GIP, Figures A2 and 3. present the spatiotemporal comparative heat map and the changing trends, respectively.

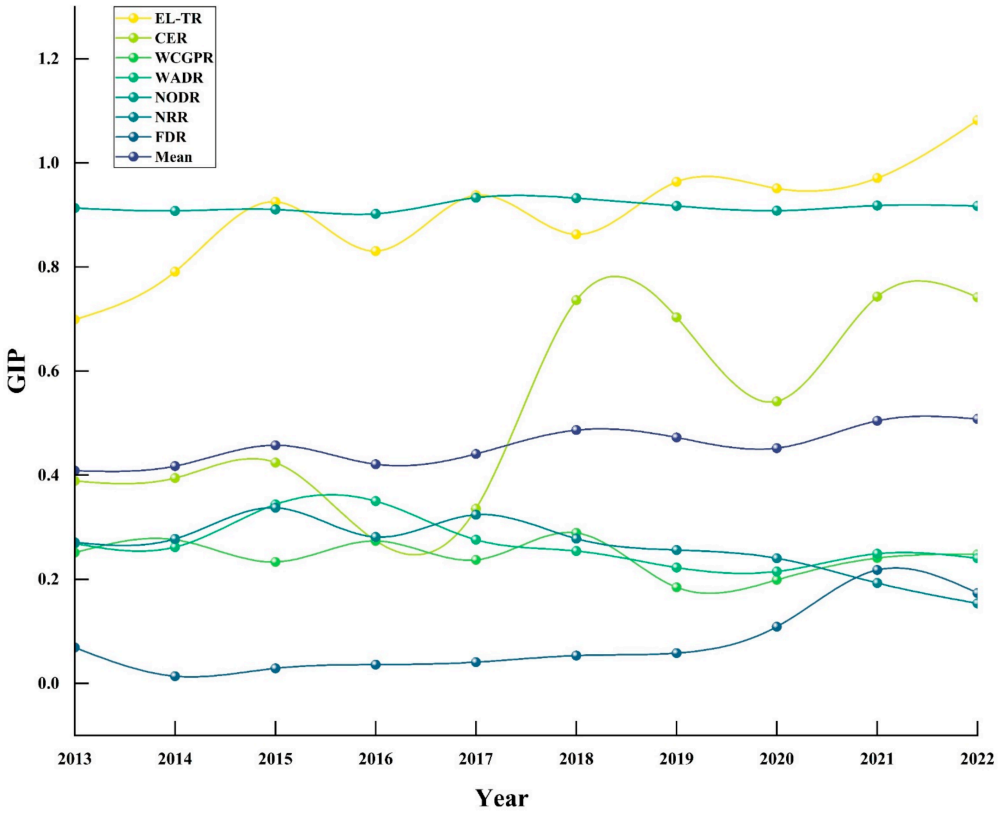


Figure 3. Evolution of logistics GIP across the seven functional regions, 2013–2022.

As shown in Figures A2 and 3, the seven functional regions differed considerably in both logistics GIP levels and temporal trajectories. Figure 3. highlights the regional trends, while Figure A2. reports the corresponding annual values. The NODR maintained the most stable high performance, fluctuating narrowly between 0.9024 and 0.9332. The EL-TR showed the strongest overall improvement, increasing from 0.6991 in 2013 to 1.0820 in 2022,

despite temporary declines in 2016 and 2018. The CER also displayed a marked catch-up pattern, rising from 0.3890 in 2013 to 0.7419 in 2022, although its trajectory remained volatile.

By contrast, the WCGPR and WADR remained at relatively low levels, reaching only 0.2479 and 0.2404, respectively, in 2022. The NRR showed a persistent downward trend, declining from 0.2709 in 2013 to 0.1535 in 2022. The FDR remained the lowest-performing region during most of the study period. Although it recovered from 0.0580 in 2019 to 0.2177 in 2021, it decreased again to 0.1733 in 2022. Overall, the regional trajectories indicate eastern leadership, central catch-up, persistent weakness in parts of western China, and continued deterioration in Northeast China.

3.1.2. Energy-Efficiency Dynamics and Decomposition of Technological Drivers of Logistics GIP

Using MATLAB R2023b, this study calculates the GML index of logistics GIP for 30 Chinese provinces and its decomposition components, including GEC, GTC, PEC, and SEC. The national annual results are reported in Table 2, while the provincial temporal evolution of the GML index is presented in Figure 4. The provincial trajectories of GEC, GTC, PEC, and SEC are reported separately in Figure A3a–d.

Table 2. GML Index and Decomposition Changes of GIP in the Logistics Industry across 30 Chinese Provinces.

Year	GEC	GTC	PEC	SEC	GML
2013–2014	1.0076	0.9837	1.0166	0.9912	0.9912
2014–2015	1.0131	0.9967	1.0096	1.0034	1.0097
2015–2016	1.0428	0.9745	1.0257	1.0168	1.0163
2016–2017	0.9916	1.0369	0.9984	0.9932	1.0282
2017–2018	0.9675	1.0301	0.9826	0.9846	0.9966
2018–2019	0.9972	1.0188	0.9868	1.0105	1.0160
2019–2020	0.9703	1.0657	0.9789	0.9912	1.0340
2020–2021	1.0205	1.0389	1.0083	1.0121	1.0602
2021–2022	1.0162	1.0344	1.0106	1.0056	1.0512
Mean	1.0030	1.0200	1.0019	1.0010	1.0226

As shown in Table 2, the GML index exhibits a fluctuating upward trend, with an average value of 1.0226, indicating an average annual growth rate of 2.26%. After 2019, the index remained above 1.03 and reached its peak of 1.0602 during 2020–2021. The average value of GTC is 1.0200, making it the main engine of growth. After a slight decline in the early period, GTC strengthened rapidly. By contrast, the average value of GEC is only 1.0030, and it declined continuously from 2016 to 2020, constrained by alternating fluctuations in PEC and SEC. Overall, logistics GIP growth was driven primarily by green technological progress, while improvements in technical efficiency remained limited. The divergence between GTC and GEC reflects a gap between technological-frontier expansion and the operational application of green technologies. Previous studies indicate that transport and logistics efficiency depends not only on technological innovation but also on infrastructure configuration, operational organization, scale coordination, and technology-absorption capacity [22,37]. Converting technological progress into efficiency gains therefore requires equipment renewal, low-carbon supporting infrastructure, multimodal coordination, and organizational adjustment. Where road-oriented assets and complementary facilities remain dominant, infrastructure path dependence may further slow the adoption of low-carbon transport modes [39–41]. Moreover, PEC and SEC remained close to unity, indicating that managerial catch-up and scale optimization contributed little to GIP growth. Thus, limited technical-efficiency improvement mainly reflects constraints in technology application, transport

organization, supporting infrastructure, and scale coordination rather than insufficient technological progress alone.

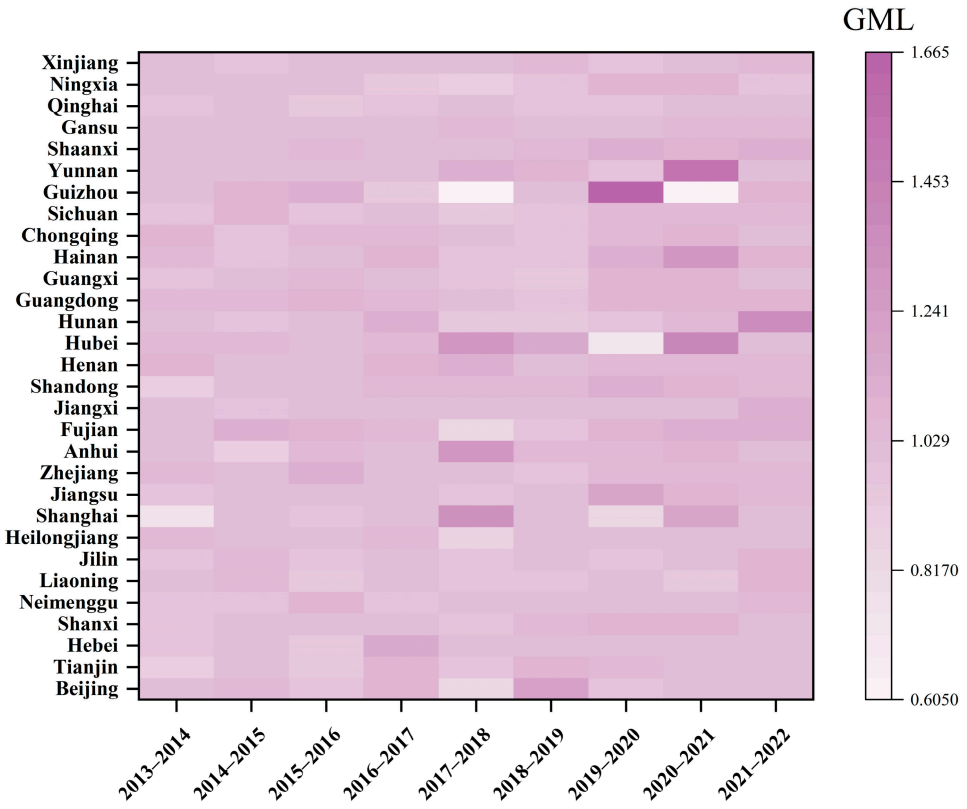


Figure 4. Provincial Temporal Evolution of the GML Index, 2013–2022.

Figure 4 presents the provincial temporal evolution of the GML index. Most provincial GML values were concentrated around unity, although substantial spatial and temporal heterogeneity remained. High-value observations became more frequent after 2019, accompanied by pronounced fluctuations in several provinces. For example, Guizhou increased to 1.6609 in 2019–2020 and then declined to 0.6096 in 2020–2021, while Yunnan reached 1.5378 in 2020–2021. The provincial trajectories of the decomposition components are reported separately in Figure A3a–d. GTC averaged 1.0200, and its national annual geometric mean remained above unity after 2016. By contrast, GEC, PEC, and SEC averaged 1.0030, 1.0019, and 1.0010, respectively, and generally fluctuated around unity. These results indicate that GML growth was driven mainly by green technological progress, while efficiency adjustment remained limited and uneven across provinces. This pattern is consistent with previous findings that converting technological progress into logistics-efficiency gains depends on operational organization and technology-absorption capacity [22,37].

3.2. Spatial Inequality and Agglomeration Characteristics of Logistics GIP

3.2.1. Source Decomposition of Spatial Inequality

This study applies the Dagum Gini coefficient to examine spatial inequality in logistics GIP and decompose its sources. Figure 5 reports the contribution rates of different disparity sources and the evolution of overall and intraregional inequality. The complete interregional Gini coefficients are presented separately in Figure A4.

As shown in Figure A4, the largest interregional disparity occurred between the Eastern Leading-Type Region and the Featured Development Region, although its Gini coefficient declined from 0.9664 in 2014 to 0.7239 in 2022. By contrast, the disparity between the Northeastern Revitalization Region and the Eastern Leading-Type Region increased

from 0.4868 in 2013 to 0.7515 in 2022. These contrasting trajectories indicate uneven regional convergence and increasing separation between the eastern leading region and Northeast China, consistent with the effects of unequal technology diffusion and infrastructure endowments identified in previous studies [31,45,46].

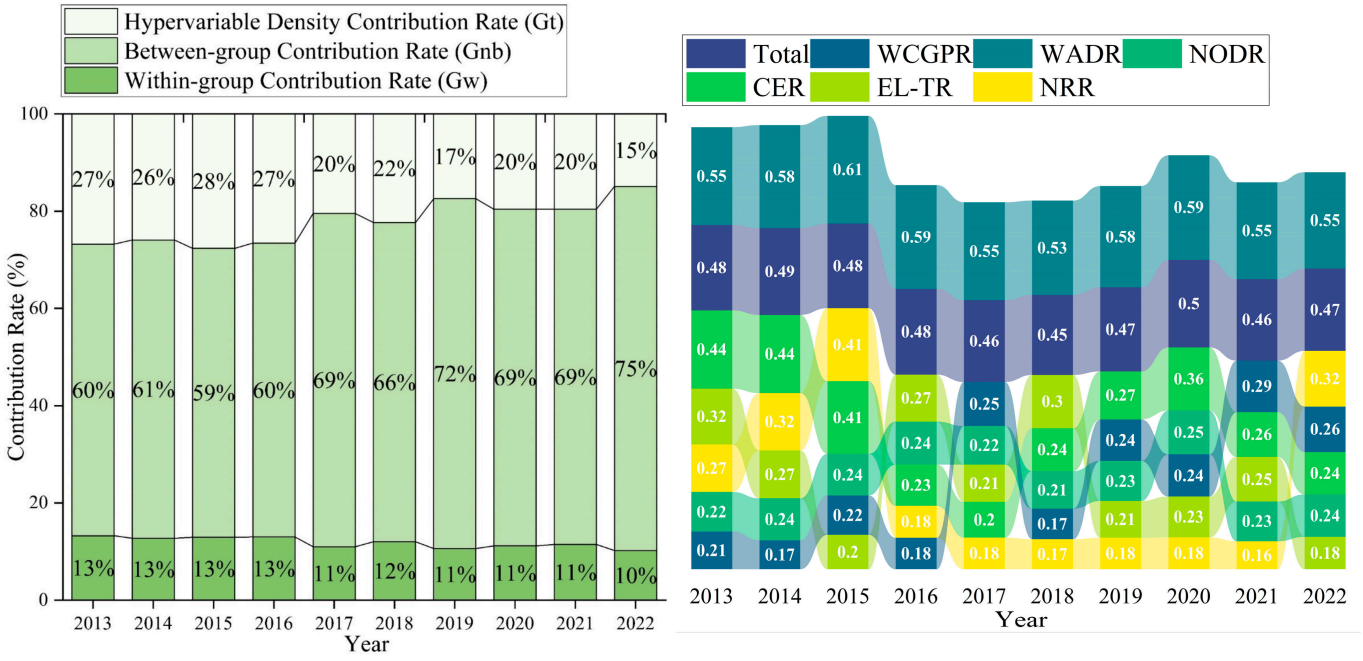


Figure 5. Dagum Gini Decomposition of Spatial Inequality in Logistics GIP, 2013–2022: (**a**) Contribution Rates of Different Disparity Sources; (**b**) Overall and Intraregional Gini Coefficients.

Figure 5a shows that the contribution of interregional disparities increased from 60% in 2013 to 75% in 2022 and remained above 65% after 2017, becoming the dominant source of spatial inequality. Meanwhile, the contributions of intraregional disparities and transvariation density declined to 10% and 15%, respectively. According to the Dagum decomposition framework, these changes indicate that national inequality increasingly originated from performance gaps between functional regions rather than differences within regions or overlaps between regional distributions [25–28].

Figure 5b further reveals substantial intraregional heterogeneity. The Western Accelerated Development Region recorded the highest internal inequality, with its Gini coefficient peaking at 0.61 in 2015 and remaining at 0.55 in 2022. In contrast, the Eastern Leading-Type Region showed stronger internal convergence, with its coefficient declining from 0.32 to 0.18. Taken together, Figures A4 and 5 demonstrate that interregional disparities gradually became the principal source of spatial inequality in logistics GIP. This pattern may be associated with regional differences in green-technology absorption, transport infrastructure endowments, and low-carbon transition capacity [31,34,45,46].

3.2.2. Global Spatial Autocorrelation

This study employs the global Moran's I index to test the spatial correlation of logistics GIP across 30 provinces based on a spatial adjacency weight matrix. As shown in Figure 6, all global Moran's I values are positive, indicating a significant positive spatial correlation. The trend showed a reversal between 2013 and 2018, while it became relatively stable from 2019 to 2022, suggesting strong spatial agglomeration characteristics.

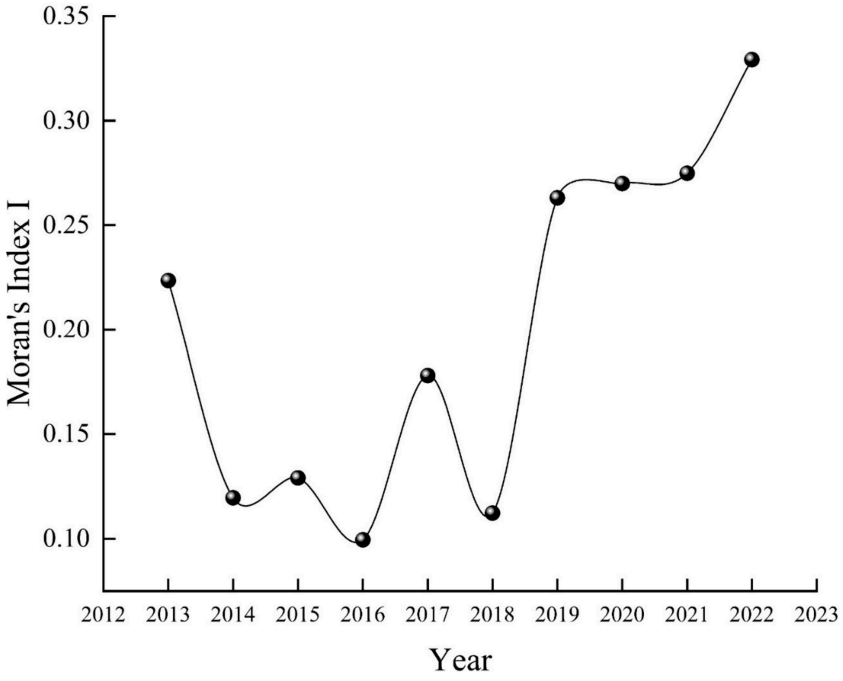


Figure 6. Changes in the global Moran's I of GIP in the logistics industry, 2013–2022.

3.2.3. Local Spatial Autocorrelation and Agglomeration Patterns

To further examine spatial agglomeration and heterogeneity, the global Moran's I results reported in Figure 6 reject the null hypothesis of spatial randomness ($p < 0.05$), confirming significant positive spatial autocorrelation in provincial logistics GIP. Based on the spatial adjacency weight matrix, local Moran's I is then used to identify local spatial association patterns. Figure 7 presents the clustering results for four representative years (2013, 2015, 2018, and 2022), while the results for the remaining years are reported in Figure A5.

As shown in Figures A5 and 7, the spatial agglomeration of logistics GIP is characterized by a stable core, peripheral adhesion, central-region upgrading, and north–south differentiation. H-H core areas such as Beijing, Tianjin, and Shanghai remained stable throughout the decade, indicating a pronounced lock-in effect. The L-L belt extending from Jilin and Heilongjiang to several southwestern provinces also showed strong persistence. Central provinces such as Anhui, Henan, and Hubei moved upward around 2018 and stabilized in the H-H quadrant, suggesting the integration of new growth poles. Guangdong remained an unchanged H-L outlier, highlighting its performance gap with surrounding areas, while Liaoning shifted from H-H to L-H, reflecting the relative decline of Northeast China. Overall, the spatial pattern has evolved from a coastal–inland divide toward a multicenter network structure. The westward expansion of H-H clusters coexists with the persistent solidification of L-L belts and L-H depressions. The consolidation and intensification of north–south disparities have become a new trend that deserves more attention than the traditional east–west divide.

The spatial evolution of logistics GIP reflects the interaction of asymmetric technology diffusion and infrastructure path dependence [45,46]. Beijing, Tianjin, and Shanghai form stable high–high clusters because of their stronger economic foundations, concentration of green innovation resources, and more developed low-carbon logistics infrastructure. However, differences in technology-absorption capacity, transport systems, and interregional coordination weaken the diffusion of technology and management experience to surrounding provinces, thereby maintaining a core–periphery structure [31,45,46]. The gradual movement of Anhui, Henan, and Hubei into high–high clusters indicates that

improved absorption capacity and stronger connections with regional innovation networks can promote the emergence of new growth poles.

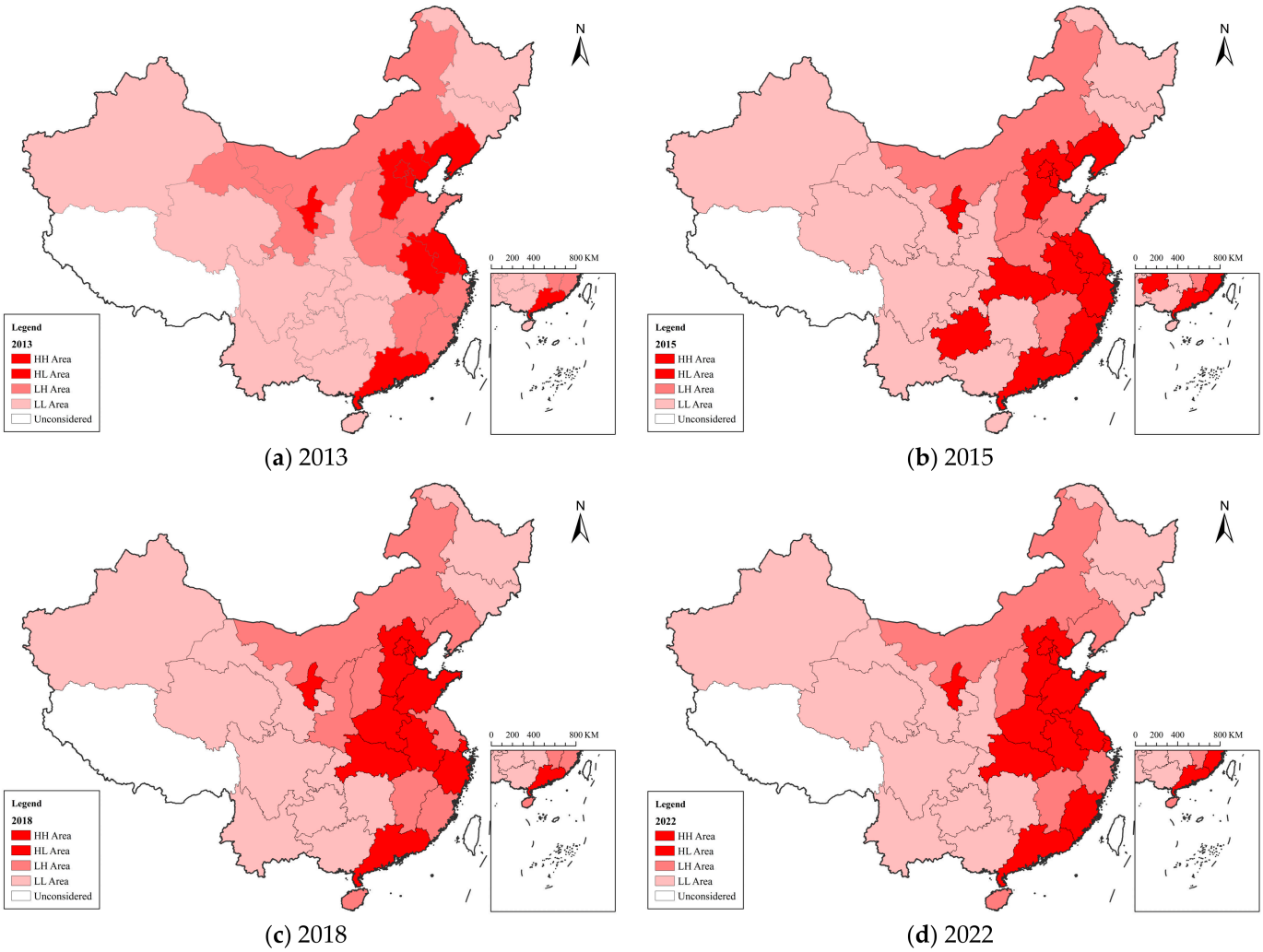


Figure 7. Local Moran's I Cluster Maps of Logistics GIP in Selected Years, 2013–2022.

By contrast, persistent low–low clusters in parts of Northeast and Southwest China are associated with weaker economic and technological foundations, dependence on road freight, and insufficient railway, multimodal, and new-energy freight infrastructure [28,39–41,47]. Existing transport assets and complementary facilities reinforce the original freight structure and increase the cost of low-carbon transition, resulting in persistent low-performance spatial lock-in [39–41]. Previous studies also associate regional differences in transport carbon performance with variations in economic capacity, technological accumulation, and infrastructure endowments [26,32]. The uneven spatial distribution of these conditions contributes to the simultaneous expansion of high-performance clusters, consolidation of low-performance areas, and widening north–south differentiation.

3.3. Transition Mechanism Analysis of Logistics GIP and Carbon Lock-In

To further reveal the formation mechanisms of logistics GIP and carbon lock-in, this study constructs a transition-mechanism variable system from six dimensions, as follows: agglomeration pressure, development capacity, path lock-in, technological human capital, resource allocation, and green technology conversion, as shown in Table 3. Among these variables, road network density is used to characterize path dependence on transport infrastructure. When the expansion of road transport networks is not coordinated with

railway freight, multimodal transport, and new-energy freight systems, it may reinforce dependence on fuel-powered trucks and lead to infrastructure-based carbon lock-in.

Table 3. Transition mechanism variables of GIP and carbon lock-in in the logistics industry.

Mechanism Type	Factors	Unit	Variable Definition	Mechanism Explanation
Agglomeration pressure mechanism	Population density	persons/km^2	Resident population per unit built-up area	Reflects the pressure of logistics demand agglomeration, traffic congestion, and energy consumption.
Development capacity mechanism	Economic development level	yuan/person	per capita gross regional product	Reflects regional capacity for green logistics investment, energy substitution, and technology absorption.
Path lock-in mechanism	Road network density	km/km^2	Total highway mileage per unit land area	Reflects dependence on road freight and the potential high-carbon path lock-in it may induce.
Technological human-capital mechanism	R&D personnel	person-years	Full-time equivalent of all personnel engaged in R&D activities	Reflects the talent support capacity for green logistics technology R&D.
Resource allocation mechanism	R&D expenditure	10,000 yuan	Total actual expenditure on R&D activities	Reflects R&D resource input and its alignment with green transition objectives.
Green technology conversion mechanism	Green patents	items	Number of green invention patents and green utility-model patents	Reflects green technology outputs and their supporting role in the low-carbon transition of logistics.

As shown in Table 4, the factors associated with logistics GIP can be interpreted from three dimensions, as follows: infrastructure carbon lock-in, R&D conversion, and green technology support. Road network density has a significantly negative coefficient of −0.130997 (p = 0.006), suggesting that road network expansion may reinforce dependence on road freight when it is not coordinated with railway freight, multimodal transport, and new-energy freight systems. This negative relationship reflects potential infrastructure carbon lock-in characterized by persistent road-freight dependence [39–41]. R&D expenditure is negatively associated with logistics GIP at the 10% significance level ($\beta = -0.084564$, p = 0.073). This relatively weak association may be related to the time lag, investment structure, and limited efficiency in converting R&D inputs into green innovation outcomes, indicating a potential disconnect between resource input and performance improvement.

Table 4. Tobit Model Regression Results.

Factors	Regression Coefficient	Standard Error	z-Statistic	*p*-Value	Significance
Population density	0.062453	0.057879	1.08	0.281	-
Economic development level	0.099098	0.040358	2.46	0.014	**
Road network density	−0.130997	0.048114	−2.72	0.006	***
R&D personnel	0.010970	0.036474	0.30	0.764	-
R&D expenditure	−0.084564	0.047226	−1.79	0.073	*
Green patents	0.035870	0.015549	2.31	0.021	**
Constant	−0.219423	0.454121	−0.48	0.629	-

Note: ***, **, and * indicate significance at the 1%, 5%, and 10% levels, respectively.

By contrast, economic development level and green patents are positively associated with logistics GIP. Economic development level has a significantly positive coefficient of 0.099098 (p = 0.014), indicating that stronger economic foundations are associated with greater capacity for green logistics investment, technology adoption, and organizational upgrading. Green patents also have a significantly positive coefficient of 0.035870 (p = 0.021), suggesting that green technology outputs may support logistics GIP improvement and help alleviate technology-related carbon lock-in. Population density and the full-time equivalent of R&D personnel are not statistically significant, indicating that demand agglomeration and increases in R&D personnel alone do not necessarily improve GIP without corresponding improvements in energy-use patterns, transport organization, and technology conversion capacity. Overall, the results suggest that infrastructure carbon lock-in is associated with persistent road-freight dependence, while limited R&D conversion efficiency may constrain the transformation of innovation inputs into performance gains. Economic development capacity and green technology outputs provide favorable conditions for weakening carbon lock-in and advancing the green transition of the logistics industry.

3.4. Robustness Test

3.4.1. Robustness of the Super-SBM Measurement Results

To examine the potential redundancy of the two digital indicators, we first conducted correlation and multicollinearity diagnostics. The correlation coefficient between enterprise website penetration rate and informatization level is 0.0912, while their variance inflation factors are 1.695 and 3.014, respectively. Both VIF values are below the commonly adopted threshold of 5, indicating no serious redundancy or multicollinearity.

We then re-estimated logistics GIP after excluding the two digital indicators while keeping the data, Super-SBM model, and estimation procedure unchanged. As shown in Table A2, the pooled Pearson and Spearman correlations between the 22-indicator baseline results and the 20-indicator results are 0.9561 and 0.9579, respectively. The mean annual absolute change in provincial rankings is only 1.33 positions. Therefore, excluding the two indicators does not materially alter the provincial efficiency pattern, confirming the robustness of the baseline measurement results.

3.4.2. Robustness of the GML Decomposition Results

To examine whether the GML decomposition results are driven by extreme observations, the eight aggregated input-output variables used in the GML analysis were winsorized at the 1st and 99th percentiles. GML and its decomposition components were then re-estimated using the unchanged directional-distance function, returns-to-scale assumptions, global and contemporaneous frontiers, and geometric-mean aggregation method. As shown in Table A3, the mean GML changes only from 1.0224 to 1.0204 after winsorization. The corresponding GEC and GTC values change from 1.0027 and 1.0196 to 1.0029 and 1.0174, respectively, while PEC and SEC remain close to unity. The Spearman correlations between the baseline and winsorized results range from 0.9243 to 0.9881, and the mean annual absolute change in provincial GML rankings is only 1.70 positions. Therefore, the conclusion that logistics GIP growth was mainly driven by green technological progress, whereas improvements in technical efficiency remained limited, is robust to extreme-value treatment.

3.4.3. Sensitivity Analysis of Regional Classification

To examine whether the Dagum Gini decomposition results depend on the seven-region classification, this study recalculates the decomposition using the official four-region classification. As shown in Table A4, the overall Gini coefficient remains unchanged under both classifications. The contribution of interregional disparities increases from 59.98% to 74.88%

under the seven-region classification and from 52.86% to 71.62% under the four-region classification, remaining the largest source of inequality in both cases. The Pearson and Spearman correlations between the two annual interregional contribution series are 0.9732 and 0.9394, respectively. Meanwhile, intraregional disparities and transvariation density show similar declining trends. Therefore, the main conclusions are robust to alternative regional classifications.

3.4.4. Robustness of the Tobit Regression Results

To evaluate the stability of the Tobit estimates, three alternative specifications were employed. First, the random-effects Tobit model was replaced with a pooled Tobit model with province-clustered standard errors. Second, all explanatory variables were lagged by one year to reduce concerns about contemporaneous reverse association. Third, all explanatory variables were winsorized at the 1st and 99th percentiles. As shown in Table A5, the coefficient of road network density remains negative and statistically significant in the pooled Tobit model (−0.2227), the lagged-variable model (−0.1356), and the winsorized model (−0.1336), consistent with the baseline estimate (−0.1310). Economic development also generally maintains a positive association with GIP, while the results for green patents remain positive in the baseline, lagged, and winsorized specifications. By contrast, the coefficient of R&D expenditure changes in magnitude and significance across specifications, and its negative association is therefore not sufficiently stable to support a firm conclusion of R&D resource misallocation. Overall, the negative association between road network density and GIP is robust to model replacement, temporal lagging, and extreme-value treatment. Nevertheless, these results represent conditional associations rather than causal evidence of infrastructure carbon lock-in.

3.4.5. Spatial Dependence Diagnostics for the Tobit Model

As shown in Table A6, the pooled Moran's I values of the generalized Tobit residuals are −0.060 (p = 0.502) and −0.048 (p = 0.148) under the adjacency and inverse-distance matrices, respectively. None of the annual statistics is significant at the 5% level. Therefore, no significant residual spatial dependence is detected, supporting the use of the random-effects Tobit model.

3.5. Endogeneity Test

To examine potential endogeneity arising from reverse causality between economic development, green patents, and GIP, this study employs a two-stage residual-inclusion approach. The second- and third-period lags of economic development and green patents are used as internal instruments. The first-stage regressions include the remaining explanatory variables, province effects, and year effects. The resulting residuals are then incorporated into the random-effects Tobit model. The second stage controls for year effects and is estimated with a lower censoring limit of zero and 20-point adaptive Gauss–Hermite quadrature. Owing to the lag structure, the estimation sample covers 2016–2022 and contains 210 observations from 30 provinces. Leave-one-province-out Jackknife standard errors are used to account for the two-stage estimation procedure.

As shown in Table A7, the conditional first-stage F-statistics for economic development and green patents are 15.704 and 12.381, respectively, indicating adequate instrument relevance. Table A8 reports the same-sample baseline and control-function results. The residuals of economic development and green patents are individually insignificant (p = 0.778 and p = 0.242), and their joint test yields F(2,29) = 0.998 with p = 0.381. Thus, the exogeneity null cannot be rejected, and the baseline random-effects Tobit model is retained. Nevertheless, the estimated coefficients are interpreted as conditional associations rather than causal effects.

4. Conclusions and Policy Implications

4.1. Conclusions

This study applies the PTM framework to examine logistics GIP and its carbon lock-in characteristics across 30 Chinese provinces from 2013 to 2022. The main conclusions are as follows.

(1) China's average logistics GIP increased from 0.4526 in 2013 to 0.5724 in 2022, but regional differences remained evident. The Northern Optimized Development Region recorded the highest ten-year average of 0.9160, whereas the Western Core Growth Pole Region averaged only 0.2431, and the Northeastern Revitalization Region declined to 0.1535 in 2022. This reflects a differentiated transition pattern characterized by eastern leadership, central catch-up, and persistent low performance in parts of western and northeastern China.

(2) The mean GML, GTC, and GEC indices were 1.0226, 1.0200, and 1.0030, respectively. Therefore, the growth of logistics GIP was driven mainly by green technological progress, while improvements in technical efficiency remained limited. The difference between technological progress and efficiency improvement indicates that advances in the green technology frontier have not been fully converted into improvements in energy use, transport organization, and operational efficiency.

(3) Interregional disparities were the primary source of spatial inequality, with their contribution increasing from 59.98% to 74.88%. Beijing, Tianjin, and Shanghai formed stable high–high clusters, while low–low clusters persisted in parts of Northeast and Southwest China. Anhui, Henan, and Hubei gradually became new high-value growth poles. The spatial pattern was therefore characterized by the coexistence of high-performance diffusion, persistent low-performance agglomeration, and increasing north–south differentiation.

(4) Road network density was negatively associated with logistics GIP ($\beta = -0.130997$, $p = 0.006$), reflecting potential infrastructure carbon lock-in characterized by persistent road-freight dependence. R&D expenditure showed a weaker and less stable negative association ($\beta = -0.084564$, $p = 0.073$), suggesting possible limitations in R&D conversion rather than conclusive evidence of resource misallocation. Economic development ($\beta = 0.099098$, $p = 0.014$) and green patents ($\beta = 0.035870$, $p = 0.021$) were positively associated with logistics GIP, whereas population density and R&D personnel were not statistically significant. The robustness tests generally supported the main findings.

4.2. Policy Implications

The policy implications derived from the empirical results are as follows.

(1) As GIP growth is driven mainly by green technological progress while efficiency improvement remains limited, logistics service providers should prioritize the application of green technologies in fleet renewal, route organization, and energy management. R&D support should focus on outcome conversion rather than expenditure growth alone.

(2) Given the negative association between road network density and GIP, public authorities should coordinate road investment with railway freight, multimodal transport, and new-energy freight systems to alleviate potential infrastructure carbon lock-in.

(3) The positive associations of green patents and economic development with GIP support patent commercialization, stronger technology-absorption capacity, and targeted financial and technical assistance for persistent low-performance regions. Cross-regional technology diffusion should also be strengthened.

(4) Public authorities and logistics platforms can provide carbon information, low-emission delivery options, and consolidated parcel-collection services to guide citizens toward

more sustainable consumption-related mobility. The insignificant effects of population density and R&D personnel also indicate that policy should prioritize resource-use and conversion efficiency rather than agglomeration or personnel expansion alone.

4.3. Research Limitations and Future Prospects

This study has several limitations. First, provincial data cannot capture firm-level or within-province heterogeneity, and Hong Kong, Macao, Taiwan, and Tibet were excluded because of data availability and continuity constraints. Second, differences in statistical definitions across yearbooks may affect data comparability. Third, DEA scores are relative to the selected sample, indicators, and efficiency frontier. Fourth, the lack of continuous measures of road-freight dependence, multimodal integration, and technology commercialization precluded mediation and moderation analyses. Fifth, insufficient data on freight electrification, charging infrastructure, and modal structure limited the analysis of transport restructuring and decarbonization. Finally, the Tobit and control-function models do not establish causality. Future research could combine firm- or city-level harmonized data with quasi-natural experiments or external instruments while incorporating freight electrification, charging infrastructure, modal-share indicators, and suitable mediating and moderating variables to examine the formation and transmission paths of logistics carbon lock-in.

Author Contributions: Conceptualization, H.Z. and Z.X.; methodology, Z.X. and P.W.; software, Z.X.; validation, Z.X.; formal analysis, H.Z., Z.X. and J.H.; investigation, H.Z. and Z.X.; resources, Z.X.; data curation, Z.X., P.W. and J.H.; writing—original draft preparation, H.Z. and Z.X.; writing—review and editing, H.Z. and Z.X.; visualization, Z.X.; supervision, H.Z. and Z.X.; project administration, Z.X.; funding acquisition, H.Z. All authors have read and agreed to the published version of the manuscript.

Funding: This work was supported by Ministry of Education Humanities and Social Sciences Research Program (23YJA790099),and the National Natural Science Foundation of China (71874067).

Institutional Review Board Statement: Not applicable.

Informed Consent Statement: Not applicable.

Data Availability Statement: The data that support the findings of this study are available from the corresponding author upon reasonable request.

Acknowledgments: We sincerely thank the journal's editorial team for their time and consideration of this manuscript. During the preparation of this manuscript, the authors used DeepSeek V3 solely for language polishing and improving the clarity of the text. The authors reviewed and edited all AI-assisted content and take full responsibility for the content of this publication.

Conflicts of Interest: The authors declare no conflicts of interest.

Appendix A

Table A1. Provincial composition and classification basis of the seven functional regions.

Functional Region	Provincial-Level Regions	Classification Basis and Rationale
Eastern Leading-Type Region (EL-TR)	Shanghai, Jiangsu, Zhejiang, Fujian, Shandong, and Guangdong	These coastal provinces cover major transport poles or clusters such as the Yangtze River Delta, Shandong Peninsula, west coast of the Taiwan Strait, and Guangdong. They have strong port accessibility, dense transport networks, and relatively mature logistics systems. Previous research also reports that carbon-constrained logistics efficiency generally declines from eastern to western China [37,48,53].

Table A1. *Cont.*

Functional Region	Provincial-Level Regions	Classification Basis and Rationale
Central Emerging Region (CER)	Anhui, Jiangxi, Henan, Hubei, and Hunan	These spatially contiguous inland provinces are important components of the Central China development strategy. Their logistics function is characterized by the expansion of inland transport corridors and logistics hubs and by their connecting role between eastern and western, as well as northern and southern, China [48,49].
Western Core Growth Pole Region (WCGPR)	Sichuan, Chongqing, and Shaanxi	This region contains the Chengdu–Chongqing transport pole and the Guanzhong Plain transport cluster. Chengdu, Chongqing, and Xi'an perform major gateway and logistics-hub functions and connect western China with national transport corridors [48,50,53].
Western Accelerated Development Region (WADR)	Inner Mongolia, Guangxi, Guizhou, Yunnan, Gansu, Qinghai, Ningxia, and Xinjiang	These provinces constitute the remaining western areas under the Western Development strategy. Long transport distances, uneven infrastructure accessibility, and relatively strong pressure to improve transport efficiency and reduce emissions distinguish them from the western core growth poles [22,48,50].
Northern Optimized Development Region (NODR)	Beijing, Tianjin, Hebei, and Shanxi	Beijing, Tianjin, and Hebei constitute an integrated northern transport system, while adjacent Shanxi has important energy-freight functions and faces distinctive pressure for energy restructuring. This grouping captures the coexistence of strong hub connectivity and the need to optimize freight and energy structures [48,53,54].
Northeastern Revitalization Region (NRR)	Liaoning, Jilin, and Heilongjiang	These provinces constitute the core area of the national Northeast Revitalization strategy. They share an established industrial and transport base but also face common challenges involving industrial restructuring, logistics modernization, and low-carbon transition [22,48,51].
Featured Development Region (FDR)	Hainan	Hainan is treated as a separate functional region because its island geography, dependence on maritime and air transportation, and free-trade-port policy produce a logistics structure that differs substantially from that of contiguous mainland provinces [48,52].

Table A2. Robustness Test of Logistics GIP by Excluding Two Digital Indicators.

Year	N	Pearson	Spearman	MAE	RMSE	Mean Absolute Rank Change
2013	30	0.9240	0.9751	0.0541	0.1645	1.20
2014	30	0.9953	0.9902	0.0199	0.0493	0.67
2015	30	0.8986	0.9123	0.0464	0.1731	1.80
2016	30	0.9952	0.8919	0.0162	0.0383	1.93
2017	30	0.9293	0.9279	0.0274	0.1083	1.60
2018	30	0.9993	0.9671	0.0045	0.0099	1.20
2019	30	0.9384	0.9657	0.0297	0.1107	1.33
2020	30	0.9197	0.9697	0.0402	0.1475	1.33
2021	30	0.9992	0.9729	0.0100	0.0182	1.27
2022	30	0.9960	0.9760	0.0177	0.0408	1.00
Pooled sample	300	0.9561	0.9579	0.0266	0.1043	1.33

Note: The pooled row reports pooled Pearson and Spearman correlations, pooled MAE and RMSE, and the mean annual absolute change in within-year provincial rankings.

Table A3. Robustness Test of the GML Decomposition Results Based on Winsorization.

Index	Baseline Mean	Winsorized Mean	Pearson	Spearman	MAE	RMSE
GML	1.0224	1.0204	0.8169	0.9407	0.0142	0.0554
GEC	1.0027	1.0029	0.9905	0.9492	0.0034	0.0128
GTC	1.0196	1.0174	0.8523	0.9254	0.0147	0.0554
PEC	1.0018	1.0021	0.9989	0.9881	0.0010	0.0038
SEC	1.0009	1.0008	0.9846	0.9243	0.0030	0.0112

Table A4. Sensitivity of the Dagum Gini decomposition to alternative regional classifications.

Year	Overall Gini	Seven-Region Intraregional (%)	Four-Region Intraregional (%)	Seven-Region Interregional (%)	Four-Region Interregional (%)	Seven-Region Transvariation (%)	Four-Region Transvariation (%)
2013	0.4849	13.26	23.80	59.98	52.86	26.76	23.34
2014	0.4927	12.73	22.72	61.33	54.71	25.94	22.57
2015	0.4801	12.94	22.30	59.43	52.89	27.63	24.81
2016	0.4832	12.99	23.81	60.45	56.76	26.57	19.43
2017	0.4644	11.00	20.37	68.52	63.33	20.48	16.30
2018	0.4520	12.00	22.29	65.68	59.07	22.32	18.63
2019	0.4740	10.62	19.25	71.95	66.92	17.43	13.83
2020	0.4977	11.16	19.76	69.23	66.62	19.61	13.61
2021	0.4612	11.46	20.35	69.00	67.39	19.54	12.26
2022	0.4670	10.22	18.64	74.88	71.62	14.90	9.74

Note: The four-region classification follows the National Bureau of Statistics of China. The overall Gini coefficient is invariant to regional classification because it is calculated from the same provincial observations. The remaining values are contribution rates (%).

Table A5. Robustness Checks for the Road Network Density Coefficient.

Specification	Road Coefficient	Standard Error	*p*-Value
Baseline Tobit	−0.130997	0.048114	0.006
Pooled Tobit	−0.222673	0.053381	<0.001
Lagged regressors	−0.135632	0.047262	0.004
1–99% winsorization	−0.133584	0.047716	0.005

Table A6. Spatial Dependence Diagnostics for the Tobit Generalized Residuals.

Year	Adjacency Moran's I	*p*-Value	Inverse-Distance Moran's I	*p*-Value
2013	−0.119	0.434	−0.054	0.433
2014	−0.132	0.392	−0.063	0.285
2015	−0.058	0.833	−0.054	0.480
2016	0.067	0.388	−0.032	0.931
2017	0.068	0.384	−0.043	0.769
2018	0.003	0.754	−0.012	0.421
2019	−0.169	0.238	−0.056	0.413
2020	0.042	0.521	−0.059	0.397
2021	0.040	0.505	−0.028	0.830
2022	−0.166	0.180	−0.070	0.140
Pooled	−0.060	0.502	−0.048	0.148

Table A7. First-Stage Diagnostics for the Internal Instruments.

Endogenous Variable	Internal Instruments	Conditional F-Statistic	*p*-Value	Partial R^2
Economic development level	Second- and third-period lags	15.704	<0.001	0.180
Green patents	Second- and third-period lags	12.381	<0.001	0.233

Note: The first-stage regressions control for the remaining explanatory variables, province effects, and year effects. Standard errors are clustered at the provincial level.

Table A8. Same-Sample Baseline and Control-Function Tobit Results.

Panel A. Same-Sample Baseline Tobit Model				
Factors	**Coefficient**	**Jackknife Standard Error**	**t-Statistic**	***p*-Value**
Population density	−0.019085	0.094301	−0.20	0.841
Economic development level	0.047899	0.081125	0.59	0.559
Road network density	−0.231030	0.166577	−1.39	0.176
R&D personnel	0.033274	0.050844	0.65	0.518
R&D expenditure	−0.088008	0.059707	−1.47	0.151
Green patents	0.054711	0.053202	1.03	0.312
Constant	0.809150	0.943344	0.86	0.398
Year effects	Yes	—	—	—
Observations	210	—	—	—
Provinces	30	—	—	—
Panel B. Control-Function Tobit Model				
Factors	**Coefficient**	**Jackknife Standard Error**	**t-Statistic**	***p*-Value**
Population density	−0.001775	0.095353	−0.02	0.985
Economic development level	0.018839	0.085271	0.22	0.827
Road network density	−0.275276	0.181742	−1.51	0.141
R&D personnel	0.039893	0.047789	0.83	0.411
R&D expenditure	−0.029862	0.089047	−0.34	0.740
Green patents	−0.048024	0.102152	−0.47	0.642
First-stage residual: economic development	−0.032523	0.114441	−0.28	0.778
First-stage residual: green patents	0.144658	0.121100	1.19	0.242
Constant	1.048960	1.090817	0.96	0.344
Joint residual test	$F(2, 29) = 0.998$	—	—	0.381
Year effects	Yes	—	—	—
Observations	210	—	—	—
Provinces	30	—	—	—

Note: Model (1) is re-estimated using the same 2016–2022 sample as Model (2) to ensure comparability. In Model (2), economic development level and green patents are treated as potentially endogenous, and their second- and third-period lags are used as internal instruments. Both models are random-effects Tobit models with a lower censoring limit of zero, year effects, and 20-point adaptive Gauss–Hermite quadrature. Standard errors are obtained using the leave-one-province-out Jackknife method, and *p*-values are based on the $t(29)$ distribution.

Appendix B

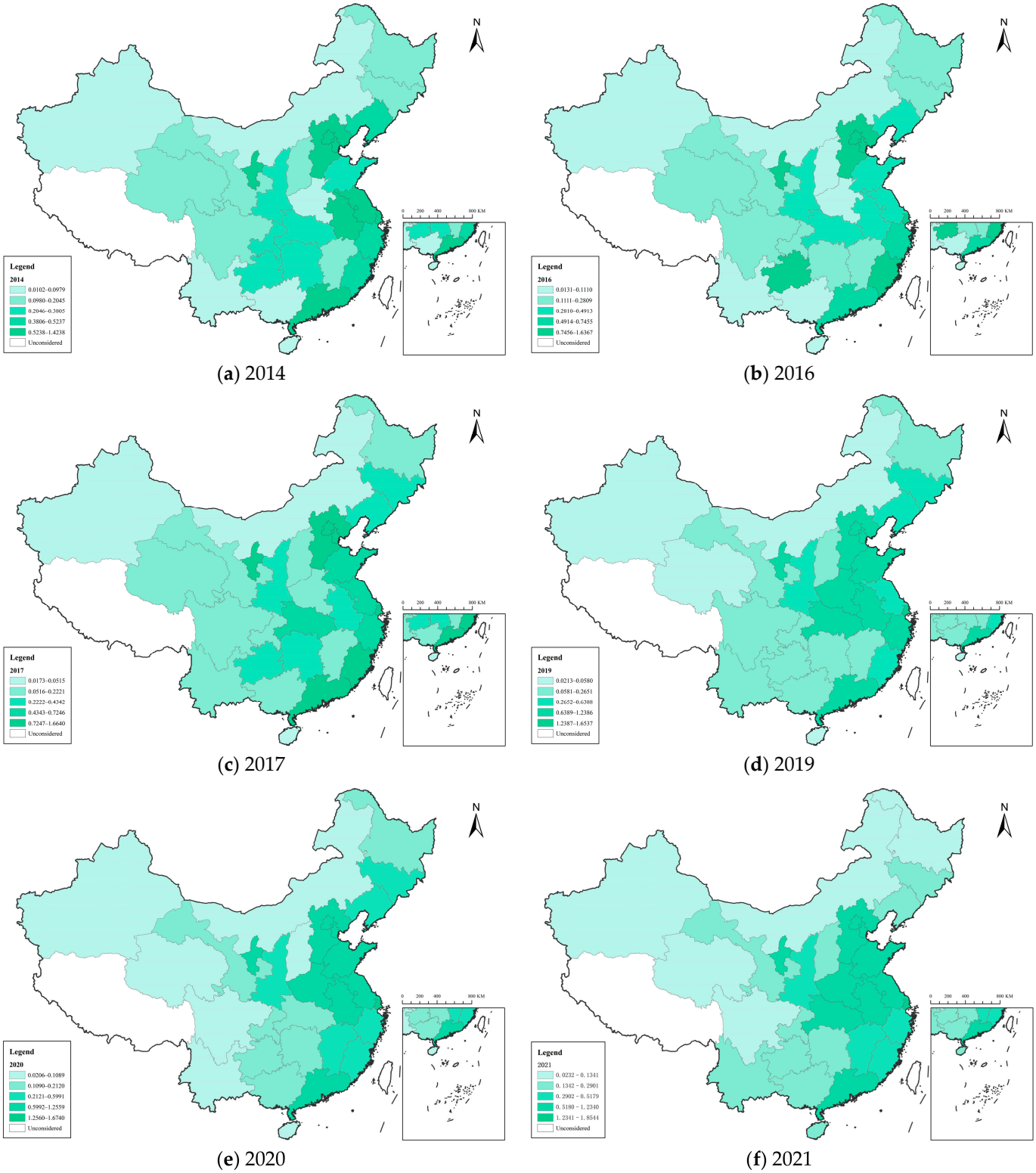


Figure A1. Provincial Spatial Distribution of Logistics GIP in the Supplementary Years.

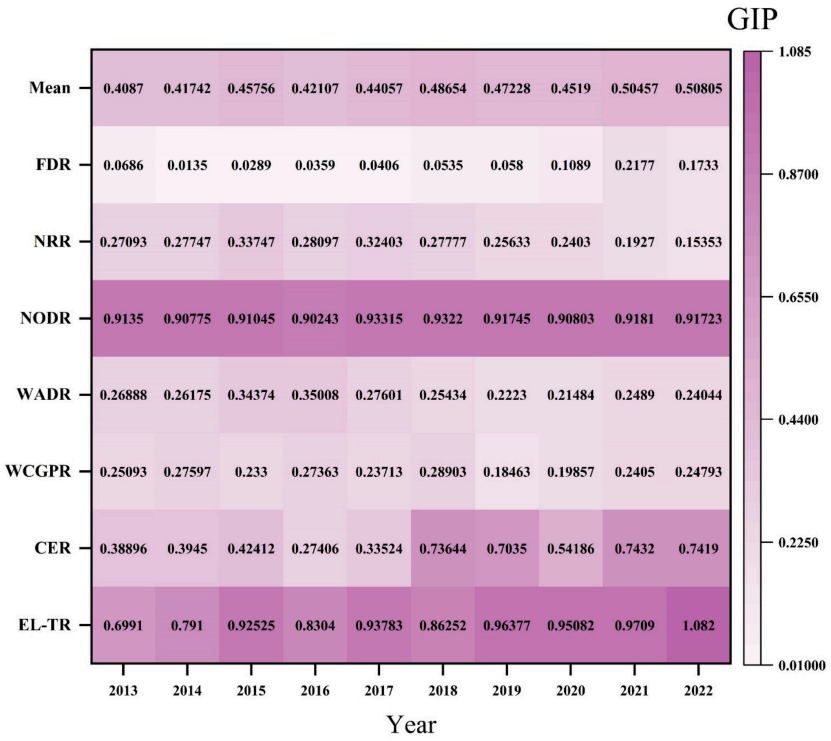


Figure A2. Spatiotemporal Heatmap of Logistics GIP across 30 Chinese Provinces, 2013–2022.

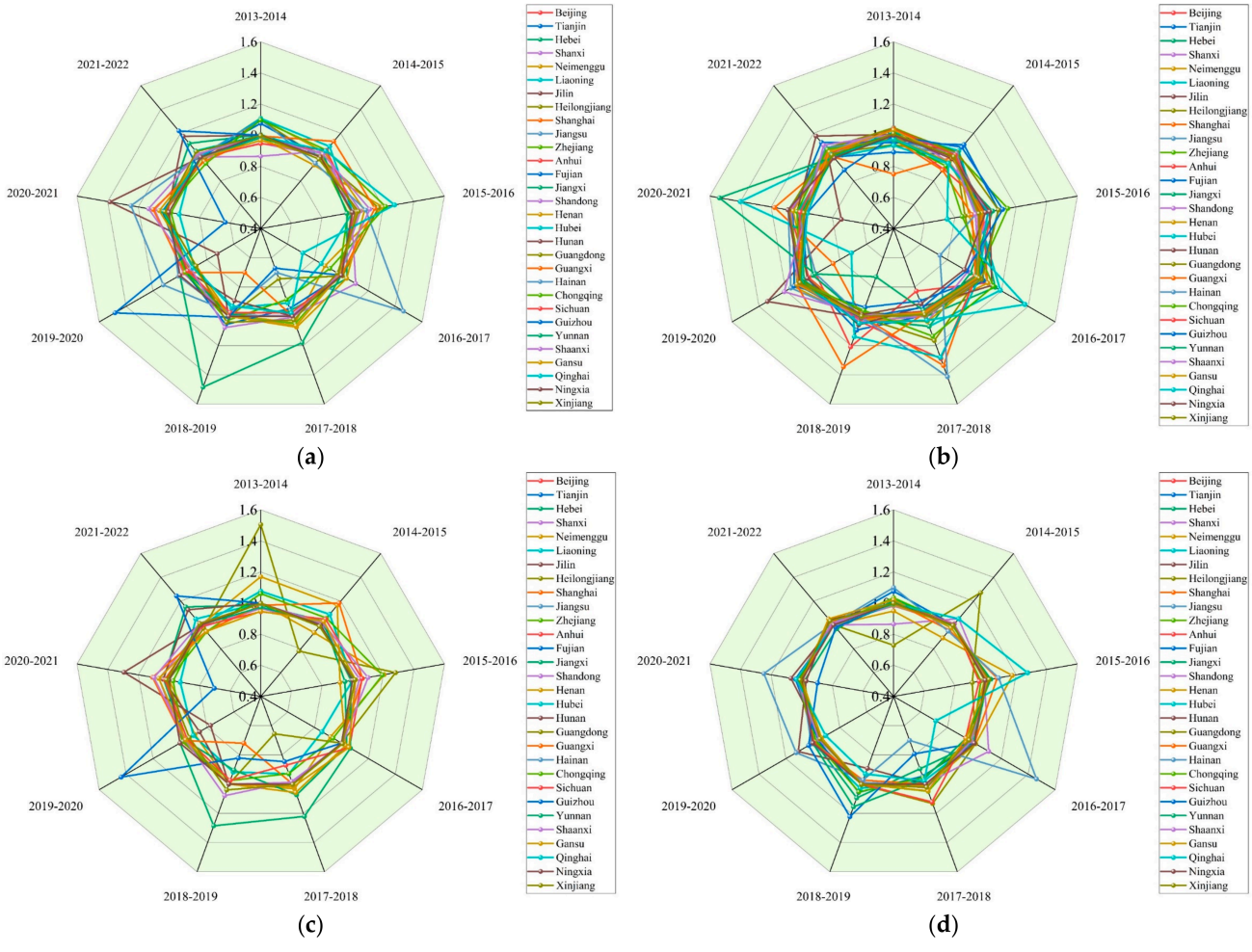


Figure A3. Provincial Temporal Dynamics of GML Decomposition Components. Note: (**a**) GEC; (**b**) GTC; (**c**) PEC; and (**d**) SEC.

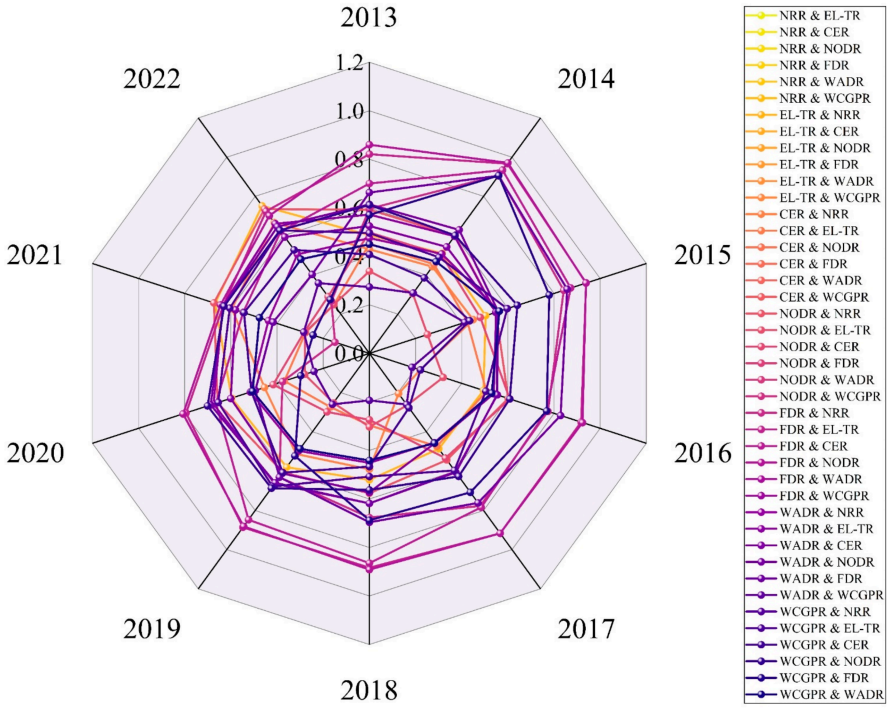


Figure A4. Temporal Evolution of Interregional Gini Coefficients for Logistics GIP, 2013–2022.

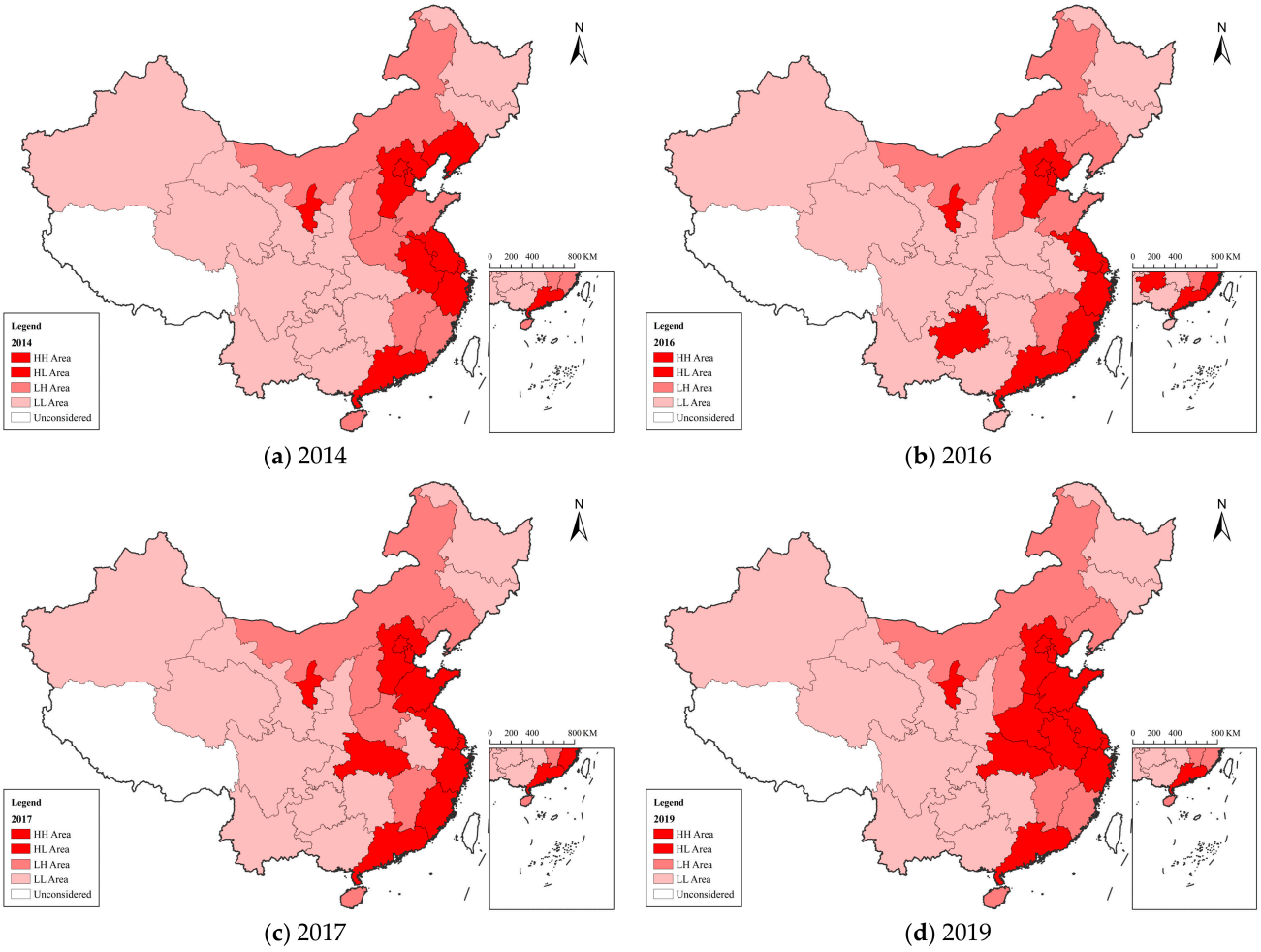
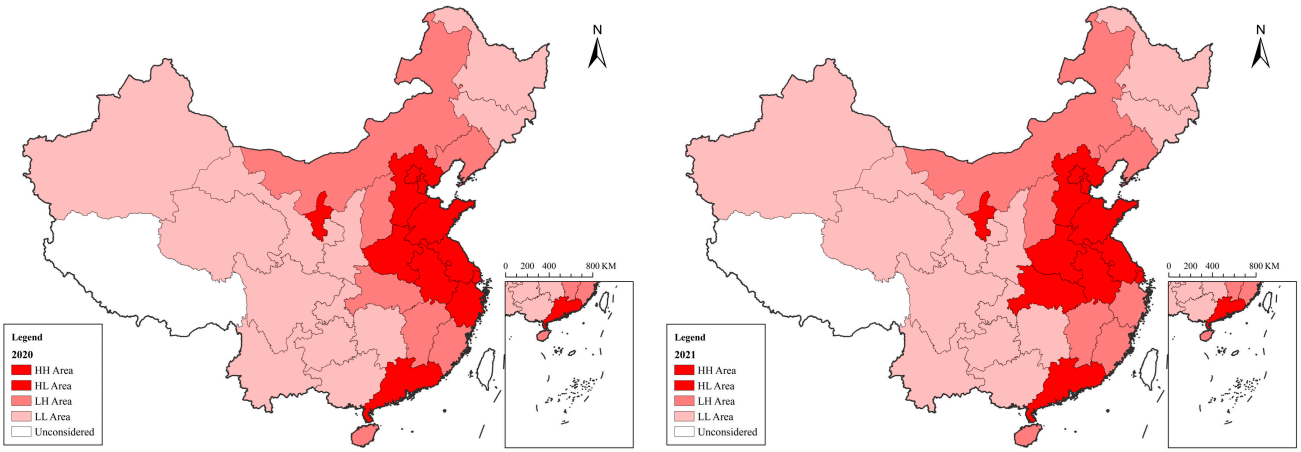


Figure A5. *Cont.*



(**e**) 2020 (**f**) 2021

Figure A5. Local Moran's I Cluster Maps of Logistics GIP in Supplementary Years.

References

1. International Energy Agency. *Global Energy Review 2025*; IEA: Paris, France, 2025. Available online: https://www.iea.org/reports/global-energy-review-2025 (accessed on 13 July 2026).
2. Intergovernmental Panel on Climate Change. Chapter 10, Transport. In *Climate Change 2022: Mitigation of Climate Change*; Cambridge University Press: Cambridge, UK, 2022. Available online: https://www.ipcc.ch/report/ar6/wg3/ (accessed on 13 July 2026).
3. Macioszek, E.; Jurdana, I. Analysis of the development of e-commerce in Poland from 2010–2020 and its impact on the transport sector. *Sci. J. Silesian Univ. Technol. Ser. Transp.* **2022**, *116*, 197–209. [CrossRef]
4. European Commission. *The European Green Deal; COM(2019) 640 Final*; European Commission: Brussels, Belgium, 2019. Available online: https://eur-lex.europa.eu/legal-content/EN/TXT/?uri=COM:2019:640:FIN (accessed on 9 August 2026).
5. United Nations General Assembly. *Transforming Our World: The 2030 Agenda for Sustainable Development*; A/RES/70/1; United Nations: New York, NY, USA, 2015. Available online: https://sdgs.un.org/2030agenda (accessed on 9 August 2026).
6. Zheng, D.; Kuroda, T. The role of public infrastructure in China's regional inequality and growth: A simultaneous equations approach. *Dev. Econ.* **2013**, *51*, 79–109. [CrossRef]
7. Lucas, K.; Mattioli, G.; Verlinghieri, E.; Guzman, A. Transport poverty and its adverse social consequences. *Proc. Inst. Civ. Eng. Transp.* **2016**, *169*, 353–365. [CrossRef]
8. Ministry of Ecology and Environment of the People's Republic of China. *China Mobile Source Environmental Management Annual Report 2025*; Ministry of Ecology and Environment: Beijing, China, 2025. Available online: https://www.mee.gov.cn/ywgz/dqhjbh/ydyhjgl/202512/t20251205_1137228.shtml (accessed on 13 July 2026).
9. International Energy Agency. *Global EV Outlook 2024*; IEA: Paris, France, 2024. Available online: https://www.iea.org/reports/global-ev-outlook-2024 (accessed on 13 July 2026).
10. International Energy Agency. *Renewables 2024: Analysis and Forecast to 2030*; IEA: Paris, France, 2024. Available online: https://www.iea.org/reports/renewables-2024 (accessed on 13 July 2026).
11. Hesselgren, M.; Ihlström, J. Stuck in the driving seat: Results from a semi-urban living lab experiment with mobility services. *J. Transp. Geogr.* **2026**, *131*, 104499. [CrossRef]
12. Dalla Longa, F.; Mulder, P.; Sterkenburg, R. Stuck in the sustainable mobility transition: A spatial analysis of transport poverty risk in the Netherlands. *J. Transp. Geogr.* **2025**, *127*, 104266. [CrossRef]
13. Wang, R.; Ren, J.; Xiang, X. Evaluating China's highway transportation efficiency based on a three-stage BAM approach and machine learning. *Alex. Eng. J.* **2026**, *141*, 257–268. [CrossRef]
14. Tone, K. A slacks-based measure of super-efficiency in data envelopment analysis. *Eur. J. Oper. Res.* **2002**, *143*, 32–41. [CrossRef]
15. Wu, J.; Wang, S.; Zhang, R.; Zhao, M.; Sun, X.; Qie, X.; Wang, Y. Measurement of green innovation efficiency in Chinese listed energy-intensive enterprises based on the three-stage Super-SBM model. *Int. Rev. Econ. Financ.* **2025**, *97*, 103819. [CrossRef]
16. Zhao, R.; Yu, X.; Zhou, X.; Deng, L.; Pu, L.; Fang, J. Evaluating carbon efficiency across the lithium-ion battery industry using a SMOTE-augmented Super-SBM approach. *Environ. Res.* **2026**, *300*, 124475. [CrossRef] [PubMed]
17. Oh, D. A global Malmquist–Luenberger productivity index. *J. Product. Anal.* **2010**, *34*, 183–197. [CrossRef]
18. Hamid, S.; Wang, Q.; Wang, K. The spatiotemporal dynamic evolution and influencing factors of agricultural green total factor productivity in Southeast Asia (ASEAN-6). *Environ. Dev. Sustain.* **2025**, *27*, 2469–2493. [CrossRef]

19. Ge, J.; Huang, Q.; Su, T. How enterprise intelligence impacts green development efficiency: Evidence from industrial robot applications. *J. Clean. Prod.* **2025**, *522*, 146396. [CrossRef]
20. Yi, R.; Chen, Y.; Chen, A. Integrating justice into the assessment of urban disaster resilience construction efficiency: Considering the undesirable welfare losses of vulnerable groups. *J. Environ. Manag.* **2025**, *394*, 127419. [CrossRef] [PubMed]
21. Liu, C.; Sun, W.; Wu, J. Synergistic effects of manufacturing spatial agglomeration and carbon emission efficiency in urban hierarchies: Evidence from the Yangtze River Delta, China. *Energy* **2026**, *359*, 141130. [CrossRef]
22. Meng, C.; Du, X.; Zhu, M.; Ren, Y.; Fang, K. The static and dynamic carbon emission efficiency of the transport industry in China. *Energy* **2023**, *274*, 127297. [CrossRef]
23. Addis, A.K. Sustainability and efficiency analysis of 42 countries: Super-SBM-DEA model and the GML productivity index with undesirable outputs. *Ecol. Indic.* **2025**, *177*, 113767. [CrossRef]
24. Qu, B.; Li, F.; Gao, Y. Decoding built environment impacts and regional interdependence of urban traffic emissions using interpretable deep learning. *J. Transp. Geogr.* **2026**, *130*, 104487. [CrossRef]
25. Dagum, C. A new approach to the decomposition of the Gini income inequality ratio. *Empir. Econ.* **1997**, *22*, 515–531. [CrossRef]
26. Wang, N.; Qu, Z.; Li, J.; Zhang, Y.; Wang, H.; Xi, H.; Gu, Z. Spatial–temporal patterns and influencing factors of carbon emissions in different regions of China. *Environ. Res.* **2025**, *276*, 121447. [CrossRef] [PubMed]
27. Gao, M.; Tu, X.; Li, Y. Regional relationship between urban–rural economic inequality and carbon intensity in China's counties: Unveiling the trade-off. *J. Rural Stud.* **2025**, *119*, 103799. [CrossRef]
28. Jiao, L.; Jiang, Y.; Wu, Y.; Huo, X.; Zhang, Y.; Wu, L. Analysis of regional differences, dynamic evolution, and convergence of China's transportation industry carbon emission intensity. *Environ. Dev. Sustain.* **2025**, 1–32. [CrossRef]
29. Tang, Y.; Jiang, H. Spatiotemporal evolution and spatial differentiation of carbon emission intensity in the Chinese transport sector. *Sci. Rep.* **2026**, *16*, 13547. [CrossRef] [PubMed]
30. Fan, J.; Meng, X.; Tian, J.; Xing, C.; Wang, C.; Wood, J. A review of transportation carbon emissions research using bibliometric analyses. *J. Traffic Transp. Eng. Engl. Ed.* **2023**, *10*, 878–899. [CrossRef]
31. Xiao, K.; Chen, X.; Zhang, H.; Wong, C.U.I. Green economic efficiency and coordinated development in the Bohai Rim Region: Addressing regional disparities for sustainable innovation and economic transformation. *Sustainability* **2025**, *17*, 932. [CrossRef]
32. Peng, Z.; Li, M. Carbon emissions intensity of the transportation sector in China: Spatiotemporal differentiation, trends forecasting, and convergence characteristics. *Sustainability* **2025**, *17*, 815. [CrossRef]
33. Qiu, Y.; Zhang, T.; Cao, Y.; Yin, J.; Chen, N. Impact of low-carbon city pilot policy on the status of urban transport carbon emission networks: Empirical evidence based on China's aviation, railway, and water transportation. *Sustain. Cities Soc.* **2025**, *130*, 106568. [CrossRef]
34. Li, W.; Cai, Z.; Jin, L. Urban green land use efficiency of resource-based cities in China: Multidimensional measurements, spatial–temporal changes, and driving factors. *Sustain. Cities Soc.* **2024**, *104*, 105299. [CrossRef]
35. Simar, L.; Wilson, P.W. Estimation and inference in two-stage, semi-parametric models of production processes. *J. Econom.* **2007**, *136*, 31–64. [CrossRef]
36. Li, Y.; Liang, J. Distributed Tobit Kalman filtering for random parameter 2-D systems: Dealing with amplify-and-forward relay and stochastic communication protocol. *Inf. Sci.* **2025**, *718*, 122355. [CrossRef]
37. Deng, F.; Xu, L.; Fang, Y.; Gong, Q.; Li, Z. PCA-DEA-Tobit regression assessment with carbon emission constraints of China's logistics industry. *J. Clean. Prod.* **2020**, *271*, 122548. [CrossRef]
38. Liu, H.; Zhang, Z.; Zhang, T.; Wang, L. Revisiting China's provincial energy efficiency and its influencing factors. *Energy* **2020**, *208*, 118361. [CrossRef] [PubMed]
39. Driscoll, P.A. Breaking carbon lock-in: Path dependencies in large-scale transportation infrastructure projects. *Plan. Pract. Res.* **2014**, *29*, 317–330. [CrossRef]
40. Dong, K.; Jia, R.; Zhao, C.; Wang, K. Can smart transportation inhibit carbon lock-in? The case of China. *Transp. Policy* **2023**, *142*, 59–69. [CrossRef]
41. Zhang, Y.; Chen, Y.; Li, K.; Wu, Y.; Ma, C. Carbon lock-in mechanisms in transport infrastructure and temporal–spatial dynamics. *Buildings* **2025**, *15*, 1714. [CrossRef]
42. Hao, Y.; Gai, Z.; Wu, H. How do resource misallocation and government corruption affect green total factor energy efficiency? Evidence from China. *Energy Policy* **2020**, *143*, 111562. [CrossRef]
43. Wang, W.; Wang, J.; Wu, H. The impact of energy-consuming rights trading on green total factor productivity in the context of the digital economy: Evidence from listed firms in China. *Energy Econ.* **2024**, *131*, 107342. [CrossRef]
44. Zhou, J.; Yang, C.; Liu, D.; Wang, Y.; Zhong, Z.; Wu, Y. A three-stage geospatial network optimal location decision model for urban green logistics centers from a sustainable perspective. *Sustain. Cities Soc.* **2025**, *128*, 106481. [CrossRef]
45. Yao, H.; Mao, H.; Zhang, S.; Wang, Z.; Wang, D.; Yang, L. The impact of environmental regulation and logistics industry agglomeration on road green logistics efficiency: Evidence from China. *Res. Transp. Econ.* **2026**, *116*, 101718. [CrossRef]

46. Yao, H.; Yu, X.; Mao, H.; Bai, D.; Zhang, S. The spatial spillover impact and transmission mechanisms of logistics agglomeration on eco-efficiency: A case study in China. *Energy* **2024**, *308*, 132826. [CrossRef]
47. Moktadir, M.A.; Ren, J. Towards green logistics: An innovative decision support model for zero-emission transportation modes development. *Transp. Res. Part E Logist. Transp. Rev.* **2024**, *189*, 103648. [CrossRef]
48. Central Committee of the Communist Party of China; State Council of the People's Republic of China. Outline of the National Comprehensive Three-Dimensional Transportation Network Plan. Available online: https://www.gov.cn/zhengce/2021-02/24/content_5588654.htm (accessed on 9 August 2026). (In Chinese)
49. Central Committee of the Communist Party of China; State Council of the People's Republic of China. Opinions on Promoting High-Quality Development of the Central Region in the New Era. Available online: https://www.mee.gov.cn/zcwj/zyygwj/202107/t20210722_849674.shtml (accessed on 9 August 2026). (In Chinese)
50. Central Committee of the Communist Party of China; State Council of the People's Republic of China. Guiding Opinions on Promoting the Formation of a New Pattern in Western Development in the New Era. Available online: https://www.gov.cn/zhengce/2020-05/17/content_5512456.htm (accessed on 9 August 2026). (In Chinese)
51. Central Committee of the Communist Party of China; State Council of the People's Republic of China. Several Opinions on Comprehensively Revitalizing Northeast China and Other Old Industrial Bases. Available online: https://app.www.gov.cn/govdata/gov/201604/26/379385/article.html (accessed on 9 August 2026). (In Chinese)
52. Central Committee of the Communist Party of China; State Council of the People's Republic of China. Master Plan for the Construction of Hainan Free Trade Port. Available online: https://app.www.gov.cn/govdata/gov/202006/01/459230/article.html (accessed on 9 August 2026). (In Chinese)
53. National Development and Reform Commission; Ministry of Transport. National Logistics Hub Layout and Construction Plan. Available online: https://zfxxgk.ndrc.gov.cn/web/iteminfo.jsp?id=15953 (accessed on 9 August 2026). (In Chinese)
54. National Development and Reform Commission. Shanxi Province Actively Explores New Paths for Comprehensive Reform. Available online: https://www.ndrc.gov.cn/xwdt/ztzl/mtqcncfz/201906/t20190628_1028388.html (accessed on 9 August 2026). (In Chinese)
55. Xu, C.; Sun, G.; Kong, T. The impact of digital transformation on enterprise green innovation. *Int. Rev. Econ. Financ.* **2024**, *90*, 1–12. [CrossRef]
56. Tang, M.; Liu, Y.; Hu, F.; Wu, B. Effect of digital transformation on enterprises' green innovation: Empirical evidence from listed companies in China. *Energy Econ.* **2023**, *128*, 107135. [CrossRef]
57. Yu, L.; Xu, J.; Yuan, X. Sustainable digital shifts in Chinese transport and logistics: Exploring green innovations and their ESG implications. *Sustainability* **2024**, *16*, 1877. [CrossRef]
58. Tobin, J. Estimation of relationships for limited dependent variables. *Econometrica* **1958**, *26*, 24–36. [CrossRef]

Disclaimer/Publisher's Note: The statements, opinions and data contained in all publications are solely those of the individual author(s) and contributor(s) and not of MDPI and/or the editor(s). MDPI and/or the editor(s) disclaim responsibility for any injury to people or property resulting from any ideas, methods, instructions or products referred to in the content.